



Indian Institute of Technology Bombay

AE 305 Flight Mechanics II, 2024

Report On

Course Project

F4 Phantom II Aircraft Mechanics

Disha Gupta	210010025
Ameya Marakarkandy	21D180003
Shubhranil Chatterjee	210100144
Rohan Suresh Mekal	22B2106

Contents

1	Introduction	5
2	Aircraft Specifications	6
2.1	General Characteristics	6
2.2	Performance	6
3	Aircraft Parameters	7
4	Animation	9
5	Kinematics and Dynamics	14
5.1	States	14
5.2	System Parameters	14
5.3	Translational Motion	15
5.3.1	Kinematics	15
5.3.2	Dynamics	15
5.4	Rotational Motion	15
5.4.1	Kinematics	15
5.4.2	Dynamics	15
6	Forces and Moments	16
6.1	Gravitational Model	16
6.2	Propulsion Model	16
6.3	Aerodynamics Model	17
7	Simulink Model	18
8	Trimming on Operating Condition	19
9	Linearization	20
9.1	Longitudinal Dynamics	22
9.2	Lateral-Directional Dynamics	22
10	Dynamic Modes and Control Design Models	24
10.1	Longitudinal Dynamics	24
10.2	Lateral-Directional Dynamics	26
11	Influence of Stability Derivatives on Eigen Values	27
11.1	Longitudinal	27
11.2	Lateral - Directional	29
12	Transfer Functions	30
12.0.1	Elevator Deflection Input	30
12.0.2	Throttle setting input	30
12.0.3	Aileron Deflection Input	30
12.0.4	Rudder Deflection Input	31

13 Response to Elevator Deflection	31
13.1 Δu Response	31
13.2 $\Delta \gamma$ Response	32
13.3 α Response	32
13.4 $\Delta \theta$ Response	33
13.4.1 Long Term Response	33
13.4.2 Short Term Response	33
13.5 Δq Response	33
13.6 MATLAB Transfer Function Responses	34
14 Response to Aileron Deflection	36
14.1 Velocity Response	36
14.2 Body Angular Rates Response	37
14.3 Attitude angles Response	38
15 Conclusion	39

List of Figures

1	A U.S. Air Force QF-4E	5
2	Aircraft Animation	13
3	6DOF (Euler Angles) Simulink Block	15
4	Gravitational Forces and Moments	16
5	Propulsion Model	16
6	Aerodynamics Model	17
7	Simulation environment on Simulink	18
8	Aircraft Dynamics Block	18
9	Optimizer results	19
10	Trimmed states	19
11	Trimmed Inputs	20
12	Input matrix of linearised plant	20
13	Longitudinal State Space Model	22
14	Lateral-Directional State Space Model	22
17	Longitudinal Dynamics Pole-Zero Plot	25
18	Lateral-Directional Dynamics Pole-Zero Plot	26
19	Effect of C_{m_q} on longitudinal dynamics	27
20	Effect of C_{x_u} on longitudinal dynamics	28
21	Effect of C_{x_u} on phugoid mode dynamics	28
22	Effect of C_{l_β} on lateral-directional dynamics	29
23	Effect of C_{n_r} on lateral-directional dynamics	29
24	$\Delta u(t)$	31
25	$\Delta \gamma(t)$	32
26	$\alpha(t)$ Long Term	32
27	$\Delta \theta(t)$ Long Term	33
28	$\Delta \theta(t)$ Short Term	33
29	$\Delta q(t)$	33
30	$\Delta \delta_e(t)$	34

33	Velocity components in body frame	36
35	Body angular rate components in body frame	37
37	attitude angles	38
38	$\Delta\phi(t)$	39

1 Introduction

The McDonnell Douglas F-4 Phantom II is a 4th gen American tandem two-seat, twin-engine, all-weather, long-range supersonic jet interceptor and fighter-bomber originally developed by McDonnell Aircraft for the United States Navy. Proving highly adaptable, it entered service with the Navy in 1961 before it was adopted by the United States Marine Corps and the United States Air Force, and by the mid-1960s it had become a major part of their air arms. Phantom production ran from 1958 to 1981 with a total of 5,195 aircraft built, making it the most-produced American supersonic military aircraft in history, and cementing its position as a signature combat aircraft of the Cold War.



Figure 1: A U.S. Air Force QF-4E

Being a fighter jet many of the assumptions that we will be using, like the Small-disturbance theory would break down as it does not apply to spinning motion, stall recovery, or any other application that involves rapid maneuvers or large-amplitude oscillations that are involved in a normal mission profile of a fighter jet. Also, it has 9 hardpoints and it is intended to be used even with assymetry so the assumption of symmetry about $i^b - k^b$ plane that we generally assume will also not hold.

In this project, we have created a simulation model of the F4 Phantom Aircraft using the data provided for cruise conditions using MATLAB and Simulink. This non-linear model is then trimmed at the cruise condition and linearized about the trim. The linearized model is then converted to lateral and longitudinal state space models using similarity transformation. Lateral and Longitudinal transfer functions are then found using these state space models.

2 Aircraft Specifications

2.1 General Characteristics

- Crew: 2
- Length: 63 ft 0 in (19.2 m)
- Wingspan: 38 ft 5 in (11.7 m)
- Width: 27 ft 7 in (8.4 m) wing folded
- Height: 16 ft 5 in (5 m)
- Wing area: 530 sq ft (49.2 m²)
- Aspect ratio: 2.77
- Airfoil: NACA 0006.4–64 root, NACA 0003-64 tip
- Empty weight: 30,328 lb (13,757 kg)
- Gross weight: 41,500 lb (18,824 kg)
- Max takeoff weight: 61,795 lb (28,030 kg)
- Maximum landing weight: 36,831 lb (16,706 kg)
- Powerplant: 2 × General Electric J79-GE-17A after-burning turbojet engines, 11,905 lbf (52.96 kN) thrust each dry, 17,845 lbf (79.38 kN) with afterburner

2.2 Performance

- Maximum speed: 1,280 kn (1,470 mph, 2,370 km/h) at 40,000 ft (12,000 m)
- Maximum speed: Mach 2.23
- Cruise speed: 510 kn (580 mph, 940 km/h)
- Combat range: 370 nmi (420 mi, 680 km)
- Ferry range: 1,457 nmi (1,677 mi, 2,699 km)
- Service ceiling: 60,000 ft (18,000 m)
- Rate of climb: 41,300 ft/min (210 m/s)
- Lift-to-drag: 8.58
- Wing loading: 78 lb/sq ft (380 kg/m²)
- Thrust/weight: 0.86 at loaded weight, 0.58 at MTOW
- Takeoff roll: 4,490 ft (1,370 m) at 53,814 lb (24,410 kg)
- Landing roll: 3,680 ft (1,120 m) at 36,831 lb (16,706 kg)

3 Aircraft Parameters

The aircraft parameters were obtained from Roskam[1] for F4 Phantom II Aircraft at subsonic cruise flying conditions.

```
1 % F4 Phantom II Aircraft Parameters
2 % Author: Ameya Marakarkandy
3 % Last Updated: 04-05-24
4
5
6 % Physical parameters of airframe
7 AC.gravity = 9.81;
8 AC.mass = 17690.102;
9
10 % Inertia Matrix
11 AC.Jx = 33895.449047;
12 AC.Jy = 165680.95494;
13 AC.Jz = 189543.35107;
14 AC.Jxz = 2982.7995162;
15 AC.Jxy = 0;
16 AC.Jyz = 0;
17 AC.J = [AC.Jx, AC.Jxy, AC.Jxz; ...
18         AC.Jxy, AC.Jy, AC.Jyz; ...
19         AC.Jxz, AC.Jyz, AC.Jz];
20
21 % Wing parameters
22 AC.S = 49.2386;
23 AC.b = 11.79576;
24 AC.c = 4.8768;
25 AC.e = 0.9;
26 AC.AR = AC.b^2/AC.S;
27
28 % Gamma parameters
29 AC.Gamma = AC.Jx*AC.Jz-AC.Jxz^2;
30 AC.Gamma1 = (AC.Jxz*(AC.Jx-AC.Jy+AC.Jz))/AC.Gamma;
31 AC.Gamma2 = (AC.Jz*(AC.Jz-AC.Jy)+AC.Jxz*AC.Jxz)/AC.Gamma;
32 AC.Gamma3 = AC.Jz/AC.Gamma;
33 AC.Gamma4 = AC.Jxz/AC.Gamma;
34 AC.Gamma5 = (AC.Jz-AC.Jx)/AC.Jy;
35 AC.Gamma6 = AC.Jxz/AC.Jy;
36 AC.Gamma7 = (AC.Jx*(AC.Jx-AC.Jy)+AC.Jxz*AC.Jxz)/AC.Gamma;
37 AC.Gamma8 = AC.Jx/AC.Gamma;
38
39 % Operating/Trim Conditions
40 AC.h = 10668;
41 AC.Va = 267;
42 AC.alpha = deg2rad(2.6);
43 %AC.Q = 1382.7035;
44 %AC.rho = AC.Q*2/(AC.Va)^2;
```

```

45
46 % International Standard Atmosphere
47 AC.rho = 1.225*(1-(2.2558e-5*AC.h))^(4.22559); % Initial Air
    Density (ISA Model)
48
49 % If a dynamic ISA Model is incorporated in simulink we will be
    able to see
50 % dependence on altitude in the results
51
52 AC.Q = 0.5*AC.rho*AC.Va^2; % Initial Dynamic Pressure
53
54 %%%%%%%%%%%%%%%%%%%%%%%%%%%%%%%%%%%%%%%%%%%%%%%
55 % Aerodynamic coefficients
56
57 AC.C_L_0      = 0.100;
58 AC.C_L_alpha  = 3.750;
59 AC.C_L_q      = 1.8;
60 AC.C_L_delta_e = 0.4;
61
62 AC.C_D_0      = 0.0205;
63 AC.C_D_alpha  = 0.300;
64 AC.C_D_q      = 0.0;
65 AC.C_D_delta_e = -0.10;
66
67 AC.C_m_0      = 0.025;
68 AC.C_m_alpha  = -0.400;
69 AC.C_m_q      = -2.7;
70 AC.C_m_delta_e = -0.580;
71
72 AC.C_Y_0      = 0.0;
73 AC.C_Y_beta   = -0.68;
74 AC.C_Y_p      = 0.0;
75 AC.C_Y_r      = 0.0;
76 AC.C_Y_delta_a = 0.016;
77 AC.C_Y_delta_r = 0.095;
78
79 AC.C_ell_0     = 0.0;
80 AC.C_ell_beta  = -0.080;
81 AC.C_ell_p     = -0.240;
82 AC.C_ell_r     = 0.070;
83 AC.C_ell_delta_a = -0.042;
84 AC.C_ell_delta_r = 0.0060;
85
86 AC.C_n_0      = 0.0;
87 AC.C_n_beta   = 0.125;
88 AC.C_n_p      = -0.036;
89 AC.C_n_r      = -0.270;
90 AC.C_n_delta_a = -0.0010;

```



```

91 AC.C_n_delta_r    = -0.066;
92
93 %%%%%%%%%%%%%%%%%%%%%%%%%%%%%%%%%%%%%%%%%%
94 % Trimming the aircraft
95
96 % Operating Conditions
97 AC.pn0    = 0;           % initial North position
98 AC.pe0    = 0;           % initial East position
99 AC.pd0    = -AC.h;       % initial Down position (
    negative altitude)
100 AC.u0     = AC.Va*cos(AC.alpha); % initial velocity along body
    x-axis
101 AC.v0     = 0;           % initial velocity along body
    y-axis
102 AC.w0     = AC.Va*sin(AC.alpha); % initial velocity along body
    z-axis
103 AC.phi0   = 0;           % initial roll angle
104 AC.theta0 = AC.alpha;    % initial pitch angle
105 AC.psi0   = 0;           % initial yaw angle
106 AC.p0     = 0;           % initial body frame roll rate
107 AC.q0     = 0;           % initial body frame pitch
    rate
108 AC.r0     = 0;           % initial body frame yaw rate
109
110 % Trim control inputs
111 AC.deltaE = 0.0118078892745844;
112 AC.deltaT = 20699.2921512690;
113 AC.deltaA = 0;
114 AC.deltaR = 0;

```

4 Animation

A simple animation is created in MATLAB for visualization of the aircraft model. This is used for better visualization of the response of the aircraft to various control surface deflections and disturbances. It takes the current state of the aircraft model as the input and updates as the state keeps changing according to the modeled dynamics.

```

1 function drawAC(uu)
2     % process inputs to function
3     pn    = uu(1);       % inertial North position
4     pe    = uu(2);       % inertial East position
5     pd    = uu(3);       % inertial Down position
6     u     = uu(4);       % velocity along xb
7     v     = uu(5);       % velocity along yb
8     w     = uu(6);       % velocity along zb
9     phi   = uu(7);       % roll angle

```

```

10     theta    = uu(8);          % pitch angle
11     psi     = uu(9);          % yaw angle
12     p       = uu(10);         % roll rate
13     q       = uu(11);         % pitch rate
14     r       = uu(12);         % yaw rate
15     t       = uu(13);         % time
16
17     % define persistent variables
18     persistent uav_handle;
19     persistent Vertices
20     persistent Faces
21     persistent facecolors
22
23     % first time function is called, initialize plot and persistent
      vars
24     if t==0
25         figure(1), clf
26         [Vertices, Faces, facecolors] = defineACBody;
27         uav_handle = drawACBody(Vertices, Faces, facecolors, ...
28                                 pn, pe, pd, phi, theta,
29                                 psi, ...
30                                 [], 'normal');
31
32         title('AC')
33         xlabel('East')
34         ylabel('North')
35         zlabel('-Down')
36         view(32,47) % set the view angle for figure
37         axis([-10,10,-10,10,-10,10]);
38         grid on
39         hold on
40
41     % at every other time step, redraw base and rod
42     else
43         drawACBody(Vertices, Faces, facecolors, ...
44                     pn, pe, pd, phi, theta, psi, ...
45                     uav_handle);
46     end
47 end
48
49 %
=====
50 % drawAC
51 % return handle if 3rd argument is empty, otherwise use 3rd arg as
   handle
52 %
=====

```

```

52 %
53 function handle = drawACBody(V,F,patchcolors,...
54                             pn,pe,pd,phi,theta,psi,...
55                             handle,mode)
56 V = rotate(V', phi, theta, psi)'; % rotate AC
57 V = translate(V', pn, pe, pd)'; % translate AC
58 %V = rotate(V', phi, theta, psi)'; % rotate AC
59
60
61 % transform vertices from NED to XYZ (for matlab rendering)
62 % Rotation about x axis by -180 deg then rotation about z' by -90
    deg
63 R = [...
64     0, 1, 0;...
65     1, 0, 0;...
66     0, 0, -1;...
67     ];
68 V = V*R;
69
70 if isempty(handle)
71     handle = patch('Vertices', V, 'Faces', F,...
72                   'FaceVertexCData',patchcolors,...
73                   'FaceColor','flat',...
74                   'EraseMode', mode);
75 else
76     set(handle,'Vertices',V,'Faces',F);
77     xlim(handle.Parent, [pe-10,pe+10]);
78     ylim(handle.Parent, [pn-10,pn+10]);
79     zlim(handle.Parent, [-pd-10,-pd+10]);
80     drawnow
81 end
82 end
83
84 %%%%%%%%%%%%%%%%%%%%%%%%%%%%%%%%%%%%%%%%%%%%%%%%%%%%%%%%%%%%%%%%%%%%%%%%%
85 function XYZ=rotate(XYZ,phi,theta,psi)
86 % define rotation matrix
87 R_roll = [...
88     1, 0, 0;...
89     0, cos(phi), -sin(phi);...
90     0, sin(phi), cos(phi)];
91 R_pitch = [...
92     cos(theta), 0, sin(theta);...
93     0, 1, 0;...
94     -sin(theta), 0, cos(theta)];
95 R_yaw = [...
96     cos(psi), -sin(psi), 0;...
97     sin(psi), cos(psi), 0;...

```

```

98         0, 0, 1];
99     R = R_roll*R_pitch*R_yaw;
100     % rotate vertices
101     XYZ = R*XYZ;
102 end
103
104 %
105 %%%%%%%%%%%%%%%%%%%%%%%%%%%%%%%%%%%%%%%%%%%%%%%%%%%%%%%%%%%%%%%%%%%%%%%%%%%
106 % translate vertices by pn, pe, pd
107 function XYZ = translate(XYZ,pn,pe,pd)
108     XYZ = XYZ + repmat([pn;pe;pd],1,size(XYZ,2));
109 end
110 %
111 %%%%%%%%%%%%%%%%%%%%%%%%%%%%%%%%%%%%%%%%%%%%%%%%%%%%%%%%%%%%%%%%%%%%%%%%%%%
112 % define AC vertices and faces
113 function [V,F,colors] = defineACBody()
114     % Define the vertices (physical location of vertices)
115
116     fusel1 = 2;
117     fusel2 = 0.5;
118     fusel3 = 8;
119     fusel_w = 2;
120     wingspan = 14;
121     chord = 2;
122     htail_span = 6;
123     htail_chord = 1;
124     vtail_span = 4;
125     vtail_chord = 1.5;
126     V = [...
127         fusel1      0      0;... % point 1
128         fusel2     fusel_w/2  -fusel_w/2;... % point 2
129         fusel2    -fusel_w/2  -fusel_w/2;... % point 3
130         fusel2    -fusel_w/2   fusel_w/2;... % point 4
131         fusel2     fusel_w/2   fusel_w/2;... % point 5
132         -fusel3     0          0;... % point 6
133         -0.5,       wingspan/2,  0;...% 7
134         -0.5,       -wingspan/2,  0;...% 8
135         -(0.5+chord), -wingspan/2,  0;...% 9
136         -(0.5+chord),  wingspan/2,  0;...% 10
137         -(fusel3 - htail_chord),  vtail_span/2,  0;...%11
138         -(fusel3 - htail_chord), -vtail_span/2,  0;...%12
139         -fusel3,      -vtail_span/2,  0;...%13
140         -fusel3,      vtail_span/2,  0;...%14
141         -(fusel3 - vtail_chord), 0,          0;...%15,
142         -fusel3,      0, -vtail_span;...%16

```

```

142 ];
143
144 % AC = stlread("pioneer.stl");
145 % V = -AC.Points;
146 % F = AC.ConnectivityList;
147 % colors = [1,1,1];
148
149 % define faces as a list of vertices numbered above
150 F = [...
151     1, 2, 3, 1;... % front
152     1, 3, 4, 1;... % back
153     1, 4, 5, 1;...
154     1, 2, 5, 1;...
155     6, 2, 3, 6;...
156     6, 3, 4, 6;...
157     6, 4, 5, 6;...
158     6, 5, 2, 6;...
159     7, 8, 9, 10;...% Wing
160     11, 12, 13, 14;...% Horizontal Tail
161     15, 16, 6, 15;...% Vertical Tail
162 ];
163
164 colors = ones(length(F),3);
165 end

```

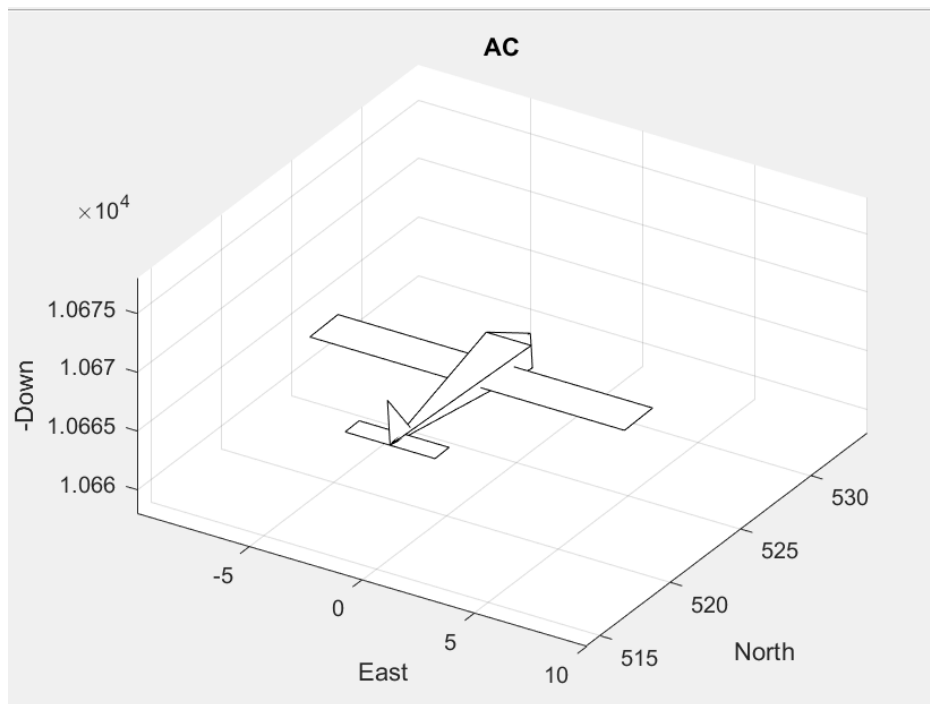


Figure 2: Aircraft Animation

5 Kinematics and Dynamics

5.1 States

A 12-state model of the aircraft was developed using Z-Y-X Brian Trait Euler angle representation, the states being:

1. p_n : x-position in NED inertial frame
2. p_e : y-position in NED inertial frame
3. p_d : z-position in NED inertial frame
4. u : x-velocity in body frame
5. v : y-velocity in body frame
6. w : z-velocity in body frame
7. ϕ : Roll angle
8. θ : Pitch angle
9. ψ : Yaw angle
10. p : Angular rate about x in body frame
11. q : Angular rate about y in body frame
12. r : Angular rate about z in body frame

5.2 System Parameters

1. m : Mass of the aircraft

2. $J = \begin{bmatrix} J_x & J_{xy} & J_{xz} \\ J_{xy} & J_y & J_{yz} \\ J_{xz} & J_{yz} & J_z \end{bmatrix}$ Moment of Inertia Matrix

Assuming symmetry about $i^b - k^b$ plane: $J_{xy} = J_{yz} = 0$

3. External forces on the aircraft: $F = \begin{bmatrix} F_x \\ F_y \\ F_z \end{bmatrix}$

External moment: $M = \begin{bmatrix} L \\ M \\ N \end{bmatrix}$

4. $\Gamma = J_x J_z - J_{xz}^2$
 $\Gamma_1 = \frac{J_{xz}(J_x - J_y + J_z)}{\Gamma}$
 $\Gamma_2 = \frac{J_z(J_z - J_y) + J_{xz}^2}{\Gamma}$
 $\Gamma_3 = \frac{J_z}{\Gamma}$
 $\Gamma_4 = \frac{J_{xz}}{\Gamma}$
 $\Gamma_5 = \frac{J_z - J_x}{J_y}$

$$\begin{aligned}\Gamma_6 &= \frac{J_{xz}}{J_y} \\ \Gamma_7 &= \frac{J_{xz}^2 + (J_x - J_y)J_x}{\Gamma} \\ \Gamma_8 &= \frac{J_x}{\Gamma}\end{aligned}$$

5.3 Translational Motion

5.3.1 Kinematics

$$\begin{bmatrix} \dot{p}_n \\ \dot{p}_e \\ \dot{p}_d \end{bmatrix} = \begin{bmatrix} \cos \theta \cos \psi & \sin \phi \sin \theta \cos \phi - \cos \phi \sin \psi & \cos \phi \sin \theta \cos \psi + \sin \phi \sin \psi \\ \cos \theta \sin \psi & \sin \phi \sin \theta \sin \psi + \cos \phi \sin \psi & \cos \phi \sin \theta \sin \psi - \sin \phi \sin \psi \\ -\sin \theta & \sin \phi \cos \theta & \cos \phi \cos \theta \end{bmatrix} \begin{bmatrix} u \\ v \\ w \end{bmatrix} \quad (1)$$

5.3.2 Dynamics

$$\begin{bmatrix} \dot{u} \\ \dot{v} \\ \dot{w} \end{bmatrix} = \begin{bmatrix} rv - qw \\ pw - ru \\ qu - pv \end{bmatrix} + \frac{1}{m} \begin{bmatrix} F_x \\ F_y \\ F_z \end{bmatrix} \quad (2)$$

5.4 Rotational Motion

5.4.1 Kinematics

$$\begin{bmatrix} \dot{\phi} \\ \dot{\theta} \\ \dot{\psi} \end{bmatrix} = \begin{bmatrix} 1 & \sin \phi \tan \theta & \cos \phi \tan \theta \\ 0 & \cos \phi & -\sin \phi \\ 0 & \sin \phi \sec \theta & \cos \phi \sec \theta \end{bmatrix} \begin{bmatrix} p \\ q \\ r \end{bmatrix} \quad (3)$$

5.4.2 Dynamics

$$\begin{bmatrix} \dot{p} \\ \dot{q} \\ \dot{r} \end{bmatrix} = \begin{bmatrix} \Gamma_1 pq - \Gamma_2 qr \\ \Gamma_5 pr - \Gamma_6 (p^2 - r^2) \\ \Gamma_7 pq - \Gamma_1 qr \end{bmatrix} + \begin{bmatrix} \Gamma_3 L + \Gamma_4 N \\ \frac{M}{J_y} \\ \Gamma_4 L + \Gamma_8 N \end{bmatrix} \quad (4)$$

Since J_{xz} is not zero there is gyroscopic roll-yaw coupling which can be observed in the simulations. By providing a moment along x-axis there is a yaw rotation and vice versa. Mathematically we can see this effect in $\Gamma_4 L$ and $\Gamma_4 N$ terms in body angular rate derivatives in z and x directions respectively where $\Gamma_4 = \frac{J_{xz}}{\Gamma}$

The Dynamics and Kinematics were modelled using the 6DOF(Euler Angles) Simulink Block available in the Simulink Aerospace Toolbox

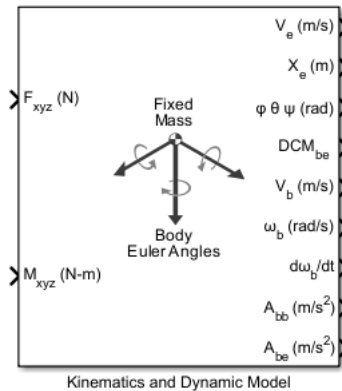


Figure 3: 6DOF (Euler Angles) Simulink Block

6 Forces and Moments

In this section, we compute forces and moments acting on the airframe of the UAV represented in the Body frame. Aerodynamic Forces are computed in the Wind Frame using the experimentally derived parameters of the airframe, Airspeed, and deflections of control surfaces.

The forces acting on an aircraft are gravitational, aerodynamic, and propulsion forces. Moments acting on the aircraft are due to aerodynamics and propulsion.

6.1 Gravitational Model

Gravity in the vehicle frame acts in the $+k$ direction. It is transformed into the body frame of the aircraft. Gravitational forces don't produce moment as our frame is centered at the centre of gravity of the aircraft.

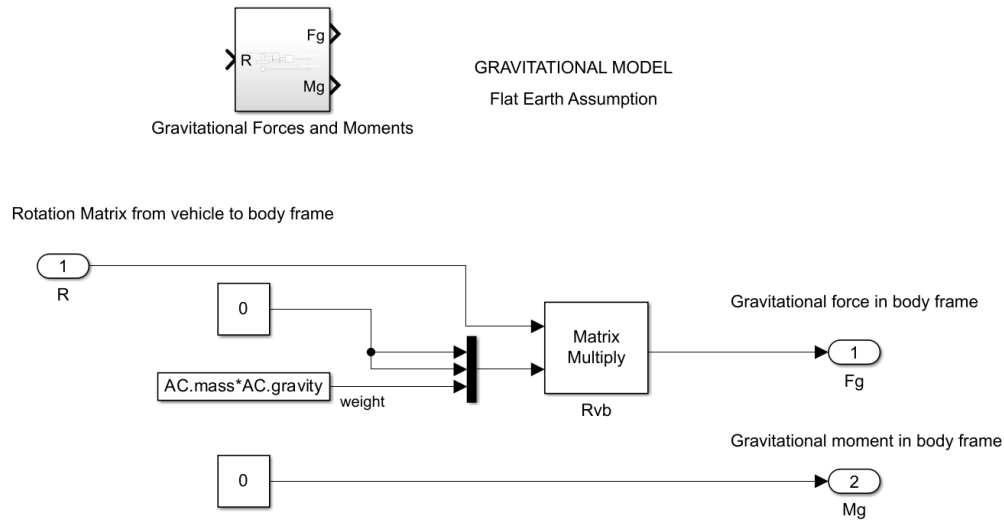


Figure 4: Gravitational Forces and Moments

6.2 Propulsion Model

For the propulsion model, we have assumed that the thrust acts exactly along the i^b direction and there is no moment produced.

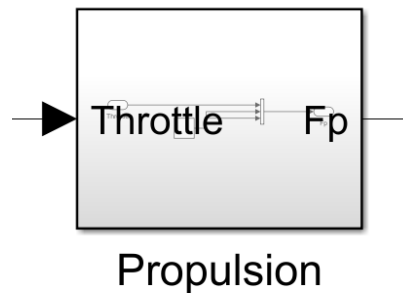


Figure 5: Propulsion Model

6.3 Aerodynamics Model

The Aerodynamics model was built using basic blocks in Simulink using the stability and control derivatives in the aircraft data available for the cruise condition.

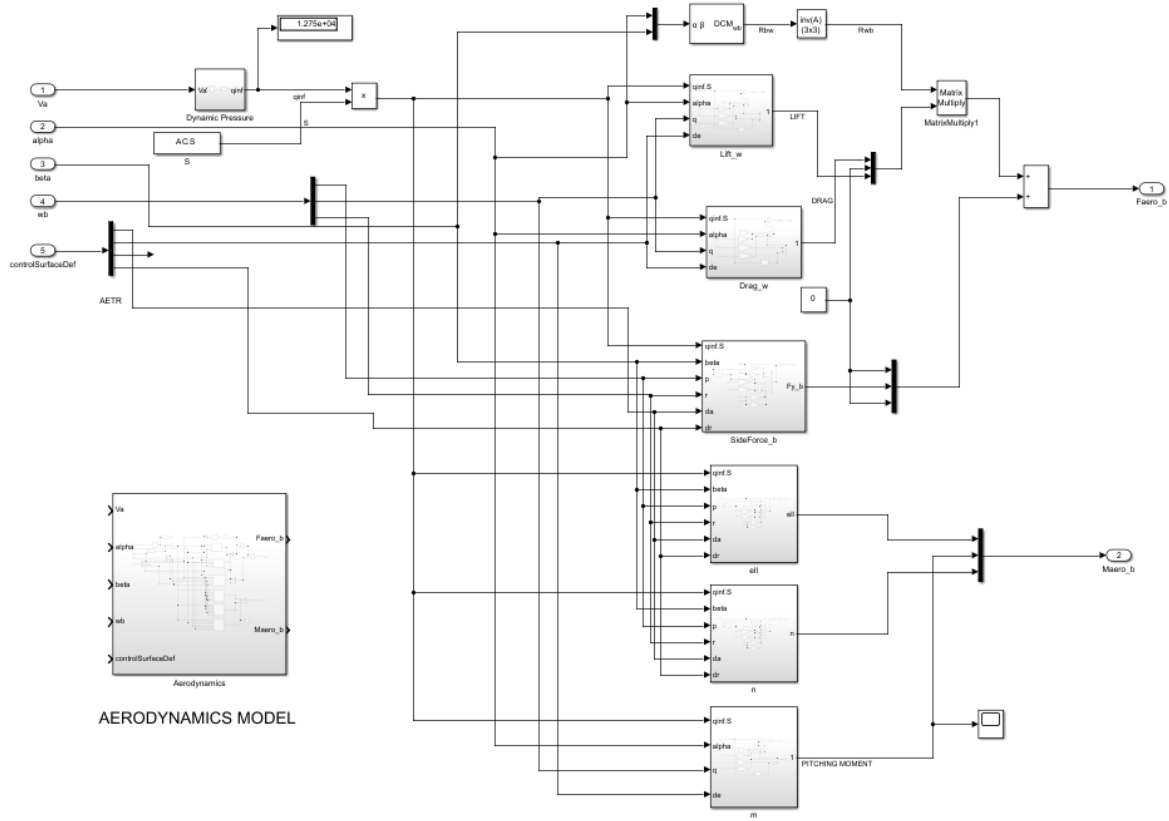


Figure 6: Aerodynamics Model

7 Simulink Model

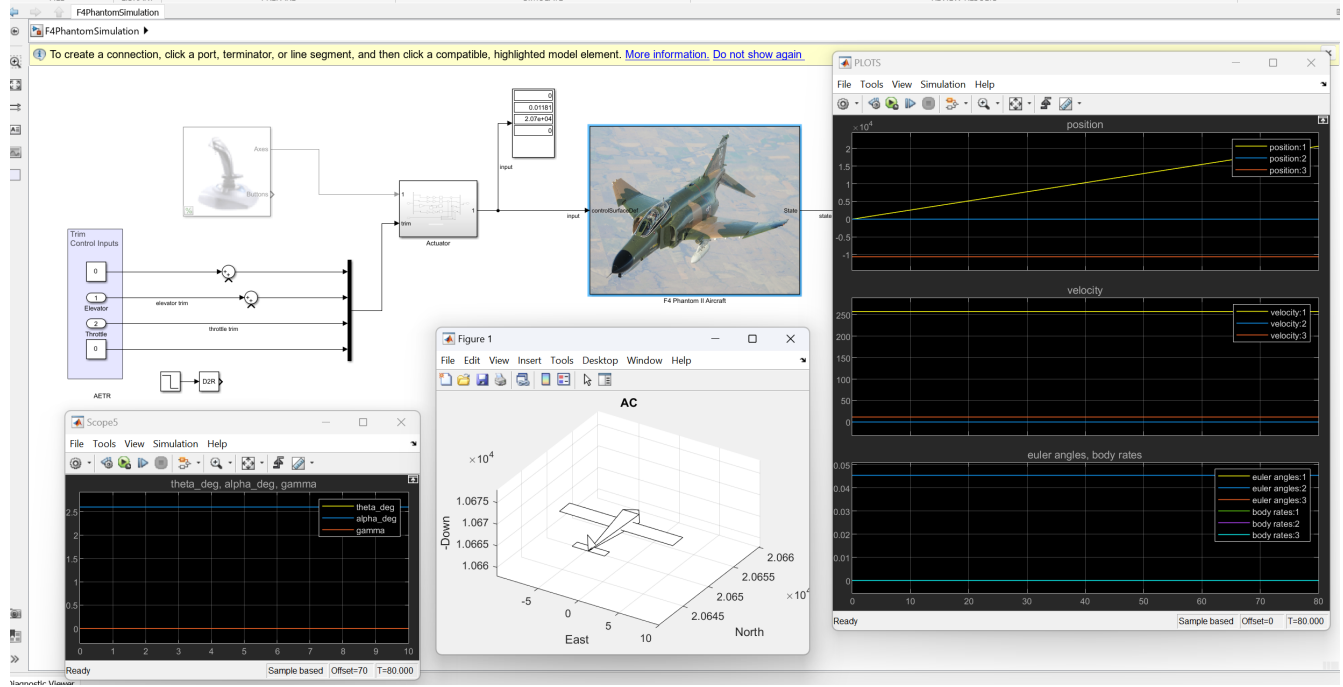


Figure 7: Simulation environment on Simulink

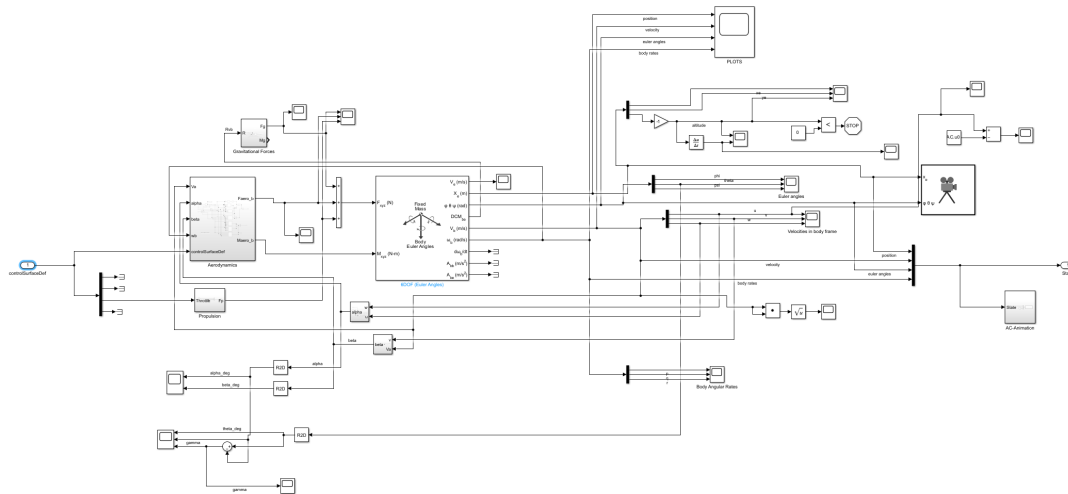


Figure 8: Aircraft Dynamics Block

8 Trimming on Operating Condition

Our operating condition is cruise flight at Velocity of 267 m/s (Mach 0.9) at an altitude of 10688 m. The air density is calculated from the International Standard Atmosphere instead of the one given in the reference.

$$C_{m_o} + C_{m_\alpha} \alpha + C_{m_{\delta_e}} = 0 \quad (5)$$

$$\delta_e = -(C_{m_o} + C_{m_\alpha} \alpha) / C_{m_{\delta_e}} \quad (6)$$

From calculation we get $\delta_e = 0.0118$

We trim the non-linear Simulink model on the operating condition using the Model Linearizer app on Simulink.

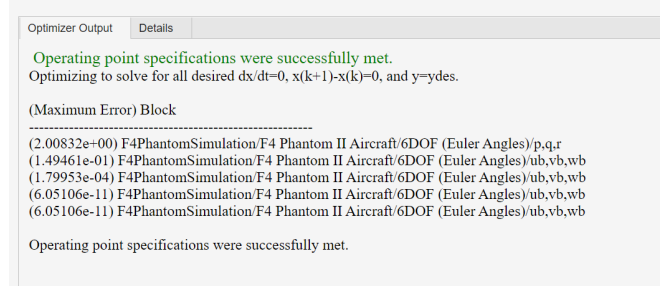


Figure 9: Optimizer results

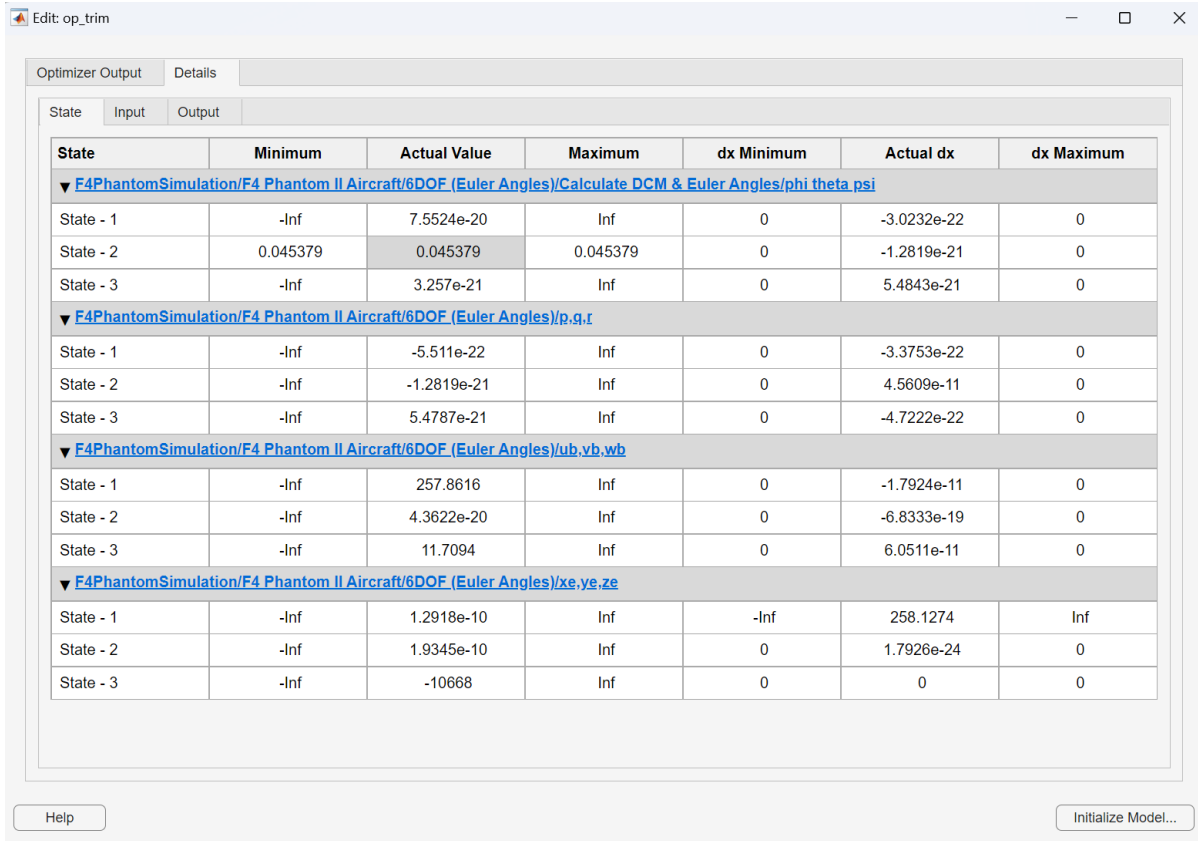


Figure 10: Trimmed states

Optimizer Output			
Details			
State	Input	Output	
Input	Minimum	Actual Value	Maximum
▼ F4PhantomSimulation/Elevator			
Input - 1	-0.2618	0.011808	0.2618
▼ F4PhantomSimulation/Throttle			
Input - 1	0	20699.2922	149244.3145

Figure 11: Trimmed Inputs

Note that the trimmed elevator deflection computed numerically by Simulink matches the analytically calculated value.

9 Linearization

Now we linearize the model at this operating condition using the Model Linearizer app. This gives us a linear state space representation of the system.

We reorder the states in the app itself to get the state space representation in the correct order as mentioned in section 5.1.

From the B matrix of the system we can notice that the longitudinal and lateral-directional states are essentially decoupled. The coupling terms are small and can be neglected.

B =					
	input(1)	input(2)	input(3)	input(4)	
xe,ye,ze(1)	0	0	0	0	
xe,ye,ze(2)	0	0	0	0	
xe,ye,ze(3)	0	0	0	0	
ub,vb,wb(1)	0	4.19	5.653e-05	0	
ub,vb,wb(2)	0.5679	5.998e-22	0	3.372	
ub,vb,wb(3)	0	-14.02	0	0	
phi theta ps	0	0	0	0	
phi theta ps	0	0	0	0	
phi theta ps	0	0	0	0	
p,q,r (1)	-9.187	0	0	1.54	
p,q,r (2)	0	-10.72	0	0	
p,q,r (3)	0.1055	0	0	-2.603	

Figure 12: Input matrix of linearised plant

Inputs are ordered as AETR conventional in RC Planes:

1. Aileron deflection
2. Elevator deflection
3. Throttle setting
4. Rudder deflection

The A matrix also shows very small coupling terms in response in states corresponding to perturbations of other states for longitudinal and lateral-directional. So we decouple the dynamics in Longitudinal and Lateral-Directional.

The decoupling is done by subjecting the system dynamics to a similarity transformation with a T matrix. This reorders the states and separates them into Longitudinal and Lateral Directional. Unwanted states are removed from the matrix and a set of 2 state space representations are obtained.

$$z = Tx$$

$$x = T^{-1}z$$

$$\dot{x} = Ax + Bu$$

$$\dot{z} = TAT^{-1}z + TBu$$

$$\dot{z} = \tilde{A}z + \tilde{B}u$$

```

1 load("linearsys.mat")
2 plant = linearsys;
3 A = plant.A;
4 B = plant.B;
5
6 % Similarity Transformation for re-ordering states
7 T=zeros(12,12);
8 T(1:3,1:3)=eye(3);
9 T(4,4) = 1;
10 T(5,6) = 1;
11 T(6,11) = 1;
12 T(7,8) = 1;
13 T(8,5) = 1;
14 T(9,10) = 1;
15 T(10,12) = 1;
16 T(11,7) = 1;
17 T(12,9) =1;
18
19 Adash = T*plant.A/T;
20 Adash(4:11,4:11); % Note Longitudinal and Lateral-Directional
    States are almost decoupled
21 Bdash = T*B;
22
23 % Longitudinal Dynamics
24 Along = Adash(4:7,4:7)
25 Blong = Bdash(4:7,2:3) % Control input AETR
26
27 % Lateral-Directional Dynamics
28 Alat = Adash(8:11,8:11)
29 Blat = Bdash(8:11,[1,4])

```

9.1 Longitudinal Dynamics

The Longitudinal states are: u, w, q, θ

Control inputs are δ_e and δ_T

	1	2	3	4
1	-0.0065	0.0199	-11.6821	-9.7999
2	-0.0523	-0.5227	257.2587	-0.4450
3	0.0013	-0.0286	-0.4714	0
4	0	0	1.0000	0

(a) A

	1	2
1	4.1897	0.0001
2	-14.0218	0
3	-10.7194	0
4	0	0

(b) B

Figure 13: Longitudinal State Space Model

Longitudinal dynamics:

$$\begin{bmatrix} \Delta \dot{u} \\ \Delta \dot{w} \\ \Delta \dot{q} \\ \Delta \dot{\theta} \end{bmatrix} = \begin{bmatrix} X_u & X_w & 0 & -g \\ Z_u & Z_w & u_0 & 0 \\ M_u + M_{\dot{w}}Z_u & M_w + M_{\dot{w}}Z_w & M_q + M_{\dot{w}}u_0 & 0 \\ 0 & 0 & 1 & 0 \end{bmatrix} \begin{bmatrix} \Delta u \\ \Delta w \\ \Delta q \\ \Delta \theta \end{bmatrix} + \begin{bmatrix} X_{\delta_e} & X_{\delta_T} \\ Z_{\delta_e} & Z_{\delta_T} \\ M_{\delta} + M_w \dot{Z}_{\delta} & M_{\delta T} + M_w \dot{Z}_{\delta T} \\ 0 & 0 \end{bmatrix} \begin{bmatrix} \Delta \delta_e \\ \Delta \delta_T \end{bmatrix}$$

9.2 Lateral-Directional Dynamics

The Lateral-Directional states are: v, p, r, ϕ

Control inputs are δ_a and δ_r

	1	2	3	4
1	-0.0980	11.7094	-257.8616	9.7999
2	-0.0695	-1.1971	0.3712	0
3	0.0200	-0.0133	-0.2469	0
4	0	1.0000	0.0454	-0.0000

(a) A

	1	2
1	0.5679	3.3719
2	-9.1866	1.5401
3	0.1055	-2.6032
4	0	0

(b) B

Figure 14: Lateral-Directional State Space Model

Lateral dynamics:

$$\begin{bmatrix} \Delta \dot{v} \\ \Delta \dot{p} \\ \Delta \dot{r} \\ \Delta \dot{\phi} \end{bmatrix} = \begin{bmatrix} Y_v & Y_p & Y_r - u_0 & g \cos \theta_0 \\ L_v & L_p & L_r & 0 \\ N_v & N_p & N_r & 0 \\ 0 & 1 & 0 & 0 \end{bmatrix} \begin{bmatrix} \Delta v \\ \Delta p \\ \Delta r \\ \Delta \phi \end{bmatrix} + \begin{bmatrix} 0 & Y_{\delta_r} \\ L_{\delta_a} & L_{\delta_r} \\ N_{\delta_a} & N_{\delta_r} \\ 0 & 0 \end{bmatrix} \begin{bmatrix} \Delta \delta_a \\ \Delta \delta_r \end{bmatrix}$$

$$\begin{pmatrix} \dot{u} \\ \dot{w} \\ \dot{q} \\ \dot{\theta} \\ \dot{h} \end{pmatrix} = \begin{pmatrix} X_u & X_w & X_q & -g \cos \theta^* & 0 \\ Z_u & Z_w & Z_q & -g \sin \theta^* & 0 \\ M_u & M_w & M_q & 0 & 0 \\ 0 & 0 & 1 & 0 & 0 \\ \sin \theta^* & -\cos \theta^* & 0 & u^* \cos \theta^* + w^* \sin \theta^* & 0 \end{pmatrix} \begin{pmatrix} \bar{u} \\ \bar{w} \\ \bar{q} \\ \bar{\theta} \\ \bar{h} \end{pmatrix} + \begin{pmatrix} X_{\delta_e} & X_{\delta_t} \\ Z_{\delta_e} & 0 \\ M_{\delta_e} & 0 \\ 0 & 0 \\ 0 & 0 \end{pmatrix} \begin{pmatrix} \delta_e^* \\ \delta_t^* \end{pmatrix}, \quad (5.51)$$

Table 5.2: Longitudinal state-space model coefficients

Longitudinal	Formula
X_u	$\frac{u^* \rho S}{m} [C_{X_0} + C_{X_\alpha} \alpha^* + C_{X_{\delta_e}} \delta_e^*] - \frac{\rho S w^* C_{X_\alpha}}{2m} + \frac{\rho S C_{X_q} u^* q^*}{4m V_a^*} + \frac{\partial T_p}{\partial u}(\delta_t^*, V_a^*)$
X_w	$-q^* + \frac{w^* \rho S}{m} [C_{X_0} + C_{X_\alpha} \alpha^* + C_{X_{\delta_e}} \delta_e^*] + \frac{\rho S C_{X_q} w^* q^*}{4m V_a^*} + \frac{\rho S C_{X_\alpha} u^*}{2m} + \frac{\partial T_p}{\partial w}(\delta_t^*, V_a^*)$
X_q	$-w^* + \frac{\rho V_a^* S C_{X_q} c}{4m}$
X_{δ_e}	$\frac{\rho V_a^{*2} S C_{X_{\delta_e}}}{2m}$
X_{δ_t}	$\frac{\partial T_p}{\partial \delta_t}(\delta_t^*, V_a^*)$
Z_u	$q^* + \frac{u^* \rho S}{m} [C_{Z_0} + C_{Z_\alpha} \alpha^* + C_{Z_{\delta_e}} \delta_e^*] - \frac{\rho S C_{Z_\alpha} w^*}{2m} + \frac{u^* \rho S C_{Z_q} q^*}{4m V_a^*}$
Z_w	$\frac{w^* \rho S}{m} [C_{Z_0} + C_{Z_\alpha} \alpha^* + C_{Z_{\delta_e}} \delta_e^*] + \frac{\rho S C_{Z_\alpha} u^*}{2m} + \frac{\rho w^* S C_{Z_q} q^*}{4m V_a^*}$
Z_q	$u^* + \frac{\rho V_a^* S C_{Z_q} c}{4m}$
Z_{δ_e}	$\frac{\rho V_a^{*2} S C_{Z_{\delta_e}}}{2m}$
M_u	$\frac{u^* \rho S c}{J_y} [C_{m_0} + C_{m_\alpha} \alpha^* + C_{m_{\delta_e}} \delta_e^*] - \frac{\rho S C_{m_\alpha} w^*}{2J_y} + \frac{\rho S c^2 C_{m_q} q^* u^*}{4J_y V_a^*}$
M_w	$\frac{w^* \rho S c}{J_y} [C_{m_0} + C_{m_\alpha} \alpha^* + C_{m_{\delta_e}} \delta_e^*] + \frac{\rho S C_{m_\alpha} u^*}{2J_y} + \frac{\rho S c^2 C_{m_q} q^* w^*}{4J_y V_a^*}$
M_q	$\frac{\rho V_a^* S c^2 C_{m_q}}{4J_y}$
M_{δ_e}	$\frac{\rho V_a^{*2} S c C_{m_{\delta_e}}}{2J_y}$

$$\begin{pmatrix} \dot{\bar{v}} \\ \dot{\bar{p}} \\ \dot{\bar{r}} \\ \dot{\bar{\phi}} \\ \dot{\bar{\psi}} \end{pmatrix} = \begin{pmatrix} Y_v & Y_p & Y_r & A_{14} & 0 \\ L_v & L_p & L_r & 0 & 0 \\ N_v & N_p & N_r & 0 & 0 \\ 0 & 1 & A_{43} & A_{44} & 0 \\ 0 & 0 & A_{53} & A_{54} & 0 \end{pmatrix} \begin{pmatrix} \bar{v} \\ \bar{p} \\ \bar{r} \\ \bar{\phi} \\ \bar{\psi} \end{pmatrix} + \begin{pmatrix} Y_{\delta_a} & Y_{\delta_r} \\ L_{\delta_a} & L_{\delta_r} \\ N_{\delta_a} & N_{\delta_r} \\ 0 & 0 \\ 0 & 0 \end{pmatrix} \begin{pmatrix} \delta_a^* \\ \delta_r^* \end{pmatrix}, \quad (5.52)$$

Table 5.1: Lateral state-space model coefficients

Lateral	Formula
Y_v	$\frac{\rho S b v^*}{4m V_a^*} [C_{Y_p} p^* + C_{Y_r} r^*] + \frac{\rho S v^*}{m} [C_{Y_0} + C_{Y_\beta} \beta^* + C_{Y_{\delta_a}} \delta_a^* + C_{Y_{\delta_r}} \delta_r^*] + \frac{\rho S C_{Y_\beta}}{2m} \sqrt{u^{*2} + w^{*2}}$
Y_p	$w^* + \frac{\rho V_a^* S b}{4m} C_{Y_p}$
Y_r	$-u^* + \frac{\rho V_a^* S b}{4m} C_{Y_r}$
Y_{δ_a}	$\frac{\rho V_a^{*2} S}{2m} C_{Y_{\delta_a}}$
Y_{δ_r}	$\frac{\rho V_a^{*2} S}{2m} C_{Y_{\delta_r}}$
L_v	$\frac{\rho S b^2 v^*}{4V_a^*} [C_{p_p} p^* + C_{p_r} r^*] + \rho S b v^* [C_{p_0} + C_{p_\beta} \beta^* + C_{p_{\delta_a}} \delta_a^* + C_{p_{\delta_r}} \delta_r^*] + \frac{\rho S b C_{p_\beta}}{2} \sqrt{u^{*2} + w^{*2}}$
L_p	$\Gamma_1 q^* + \frac{\rho V_a^* S b^2}{4} C_{p_p}$
L_r	$-\Gamma_2 q^* + \frac{\rho V_a^* S b^2}{4} C_{p_r}$
L_{δ_a}	$\frac{\rho V_a^{*2} S b}{2} C_{p_{\delta_a}}$
L_{δ_r}	$\frac{\rho V_a^{*2} S b}{2} C_{p_{\delta_r}}$
N_v	$\frac{\rho S b^2 v^*}{4V_a^*} [C_{r_p} p^* + C_{r_r} r^*] + \rho S b v^* [C_{r_0} + C_{r_\beta} \beta^* + C_{r_{\delta_a}} \delta_a^* + C_{r_{\delta_r}} \delta_r^*] + \frac{\rho S b C_{r_\beta}}{2} \sqrt{u^{*2} + w^{*2}}$
N_p	$\Gamma_7 q^* + \frac{\rho V_a^* S b^2}{4} C_{r_p}$
N_r	$-\Gamma_1 q^* + \frac{\rho V_a^* S b^2}{4} C_{r_r}$
N_{δ_a}	$\frac{\rho V_a^{*2} S b}{2} C_{r_{\delta_a}}$
N_{δ_r}	$\frac{\rho V_a^{*2} S b}{2} C_{r_{\delta_r}}$
A_{14}	$g \cos \theta^* \cos \phi^*$
A_{43}	$\cos \phi^* \tan \theta^*$
A_{44}	$q^* \cos \phi^* \tan \theta^* - r^* \sin \phi^* \tan \theta^*$
A_{53}	$\cos \phi^* \sec \theta^*$
A_{54}	$p^* \cos \phi^* \sec \theta^* - r^* \sin \phi^* \sec \theta^*$

10 Dynamic Modes and Control Design Models

For designing autopilot for the aircraft we need reduced order model of the full nonlinear 12 state model. We linearise the model at trim condition and reduce it to get a set of 2 state space models for longitudinal and lateral directional dynamics. We then find out transfer functions relating the control inputs to the states and create cascaded closed loops by successive loop closure.

The basic idea behind successive loop closure is to close several simple feedback loops in succession around the open-loop plant dynamics (1st or 2nd order) rather than designing a single (presumably more complicated) control systems.

10.1 Longitudinal Dynamics

Using the Longitudinal Dynamics system the eigen values of the A matrix can be computed which will give us the poles for the Short Period mode and the Phugoid mode

```
1 load("F4Parameters.mat")
2 load('F4LongitudinalDynamics.mat')
3 C = eye(4); D=0;
4 longsys = ss(Along,Blong,C,D);
5
6 figure;
7 title("Longitudinal Dynamics pole-zero plot")
8 pzplot(longsys,'b')
9
10 Glong = tf(longsys);
11
12 % Elevator Input
13 Ge2u = Glong(1,1);
14 Ge2w = Glong(2,1);
15 Ge2q = Glong(3,1);
16 Ge2theta = Glong(4,1);
17
18 % Throttle Input
19 Gt2u = Glong(1,2);
20 Gt2w = Glong(2,2);
21 Gt2q = Glong(3,2);
22 Gt2theta = Glong(4,2);
```

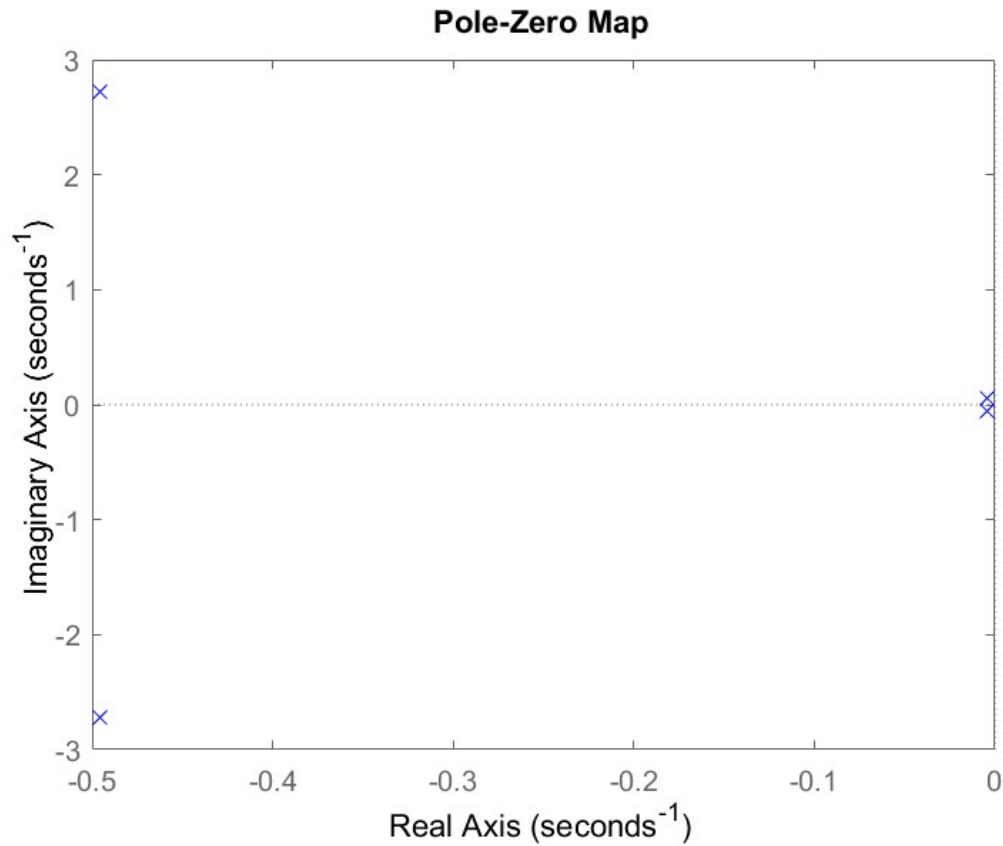



Figure 17: Longitudinal Dynamics Pole-Zero Plot

There are 2 sets of oscillatory poles as seen in the pole-zero map, All 4 are stable LHP poles. The set closer to origin (small ω_n) and with small $\zeta\omega_n$ which shows that the time period of oscillations will be large and the decay will also be slow (envelope of 2nd order response depends on $\zeta\omega_n$ term). This is the Phugoid Mode.

$$\begin{aligned} &\text{Phugoid Mode} \\ &-0.0043 + 0.0526j \\ &0.0043 - 0.0526j \end{aligned}$$

Time period = 119.45s (around 2 minutes)

The other set of poles further from the origin and the real axis belong to the Short Period mode which have a fast transient response and decay faster on perturbation.

$$\begin{aligned} &\text{Short Period Mode} \\ &-0.4960 + 2.7151j \\ &-0.4960 - 2.7151j \end{aligned}$$

Time period = 2.31s

10.2 Lateral-Directional Dynamics

Using the Lateral-Directional Dynamics system the eigen values of the A matrix can be computed which will give us the poles for the lateral-directional modes: Spiral Mode, Roll Subsidence Mode, Dutch Roll Mode

```
1 load("F4Parameters.mat")
2 load('F4LateralDynamics.mat')
3 C = eye(4); D=0;
4 latsys = ss(Alat,Blat,C,D);
5
6 figure;
7 pzplot(latsys,'r')
8
9 Glat = tf(latsys);
10
11 % Aileron Input
12 Ga2v = Glat(1,1);
13 Ga2p = Glat(2,1);
14 Ga2r = Glat(3,1);
15 Ga2phi = Glat(4,1);
16
17 % Rudder Input
18 Gr2v = Glat(1,2);
19 Gr2p = Glat(2,2);
20 Gr2r = Glat(3,2);
21 Gr2phi = Glat(4,2);
```

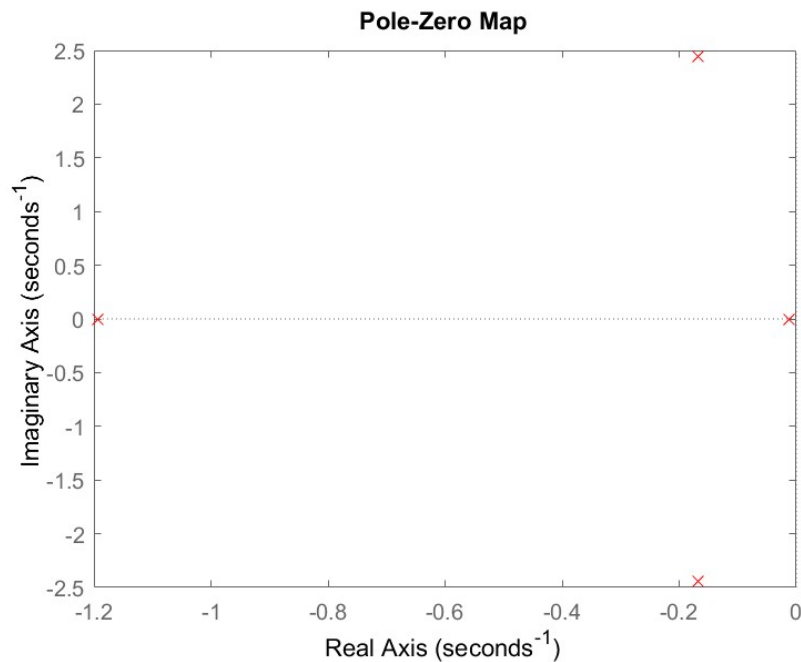


Figure 18: Lateral-Directional Dynamics Pole-Zero Plot

There are 2 non-oscillatory poles. The one further away from origin is a very stable fast pole corresponding to the roll subsidence mode. The one closer to the origin is a stable but slow pole corresponding to the Spiral mode. The oscillatory poles make up the Dutch Roll mode.

Roll Subsidence Mode

-1.1934

Spiral Mode

-0.0118

Dutch Roll Mode

$-0.1684 + 2.4431j$

$-0.1684 - 2.4431j$

11 Influence of Stability Derivatives on Eigen Values

11.1 Longitudinal

The longitudinal eigenvalues are plotted for different values of C_{m_q} in Figure 19. It can be observed that increasing the magnitude of C_{m_q} stabilizes the dynamics of the short-period mode while having no observable effect on the phugoid dynamics.

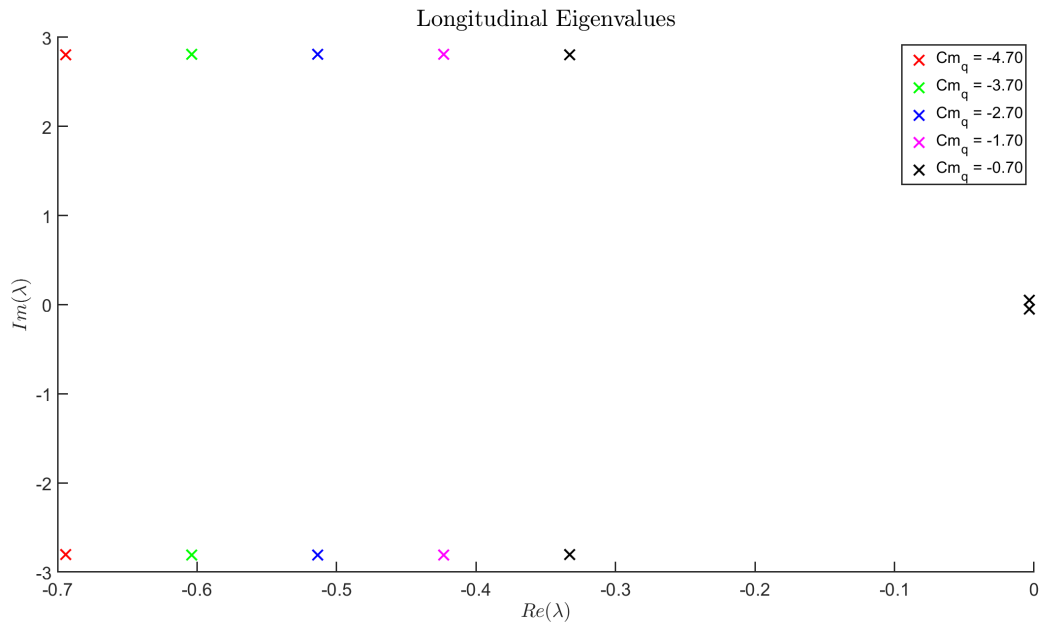


Figure 19: Effect of C_{m_q} on longitudinal dynamics

Figure 20 show the longitudinal eigenvalues for different values of C_{x_u} . At first glance, there seems to be no observable effect on any of the modes. However, a closer look in Figure 21 reveals that an increase in the magnitude of C_{x_u} stabilizes the phugoid mode dynamics.

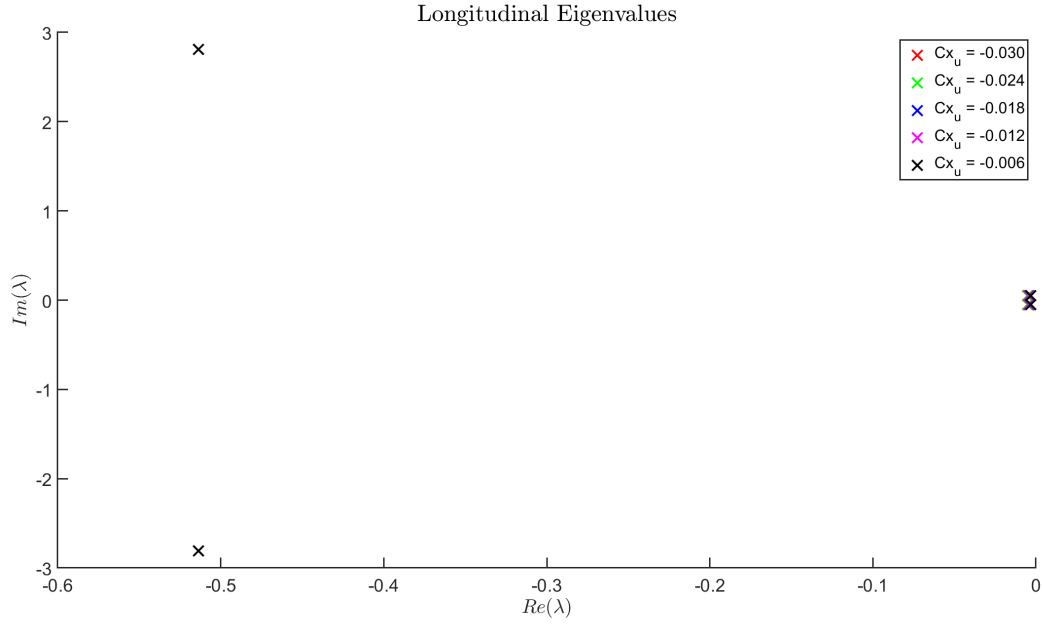


Figure 20: Effect of C_{x_u} on longitudinal dynamics

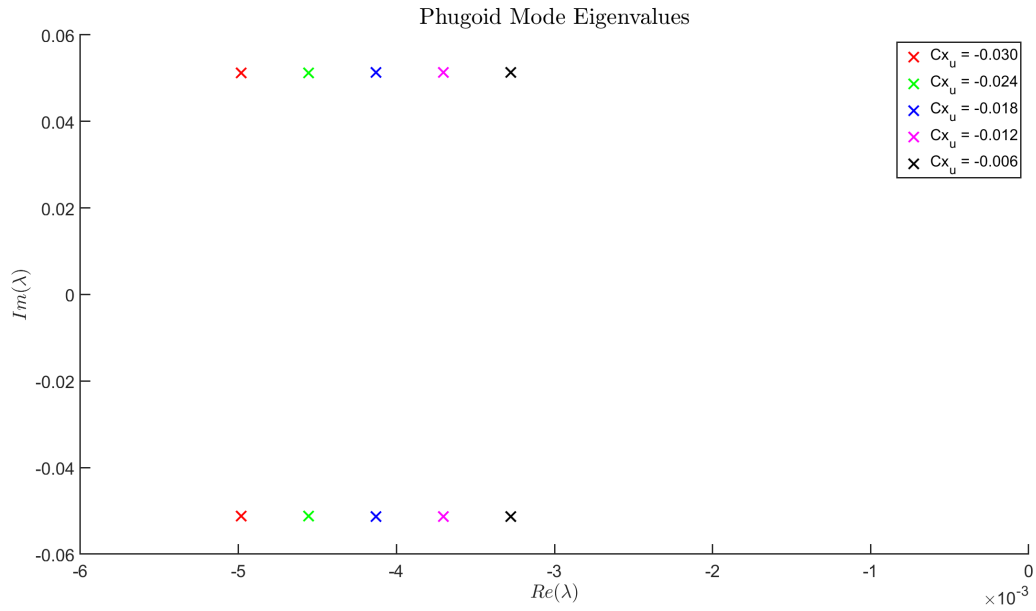


Figure 21: Effect of C_{x_u} on phugoid mode dynamics

11.2 Lateral - Directional

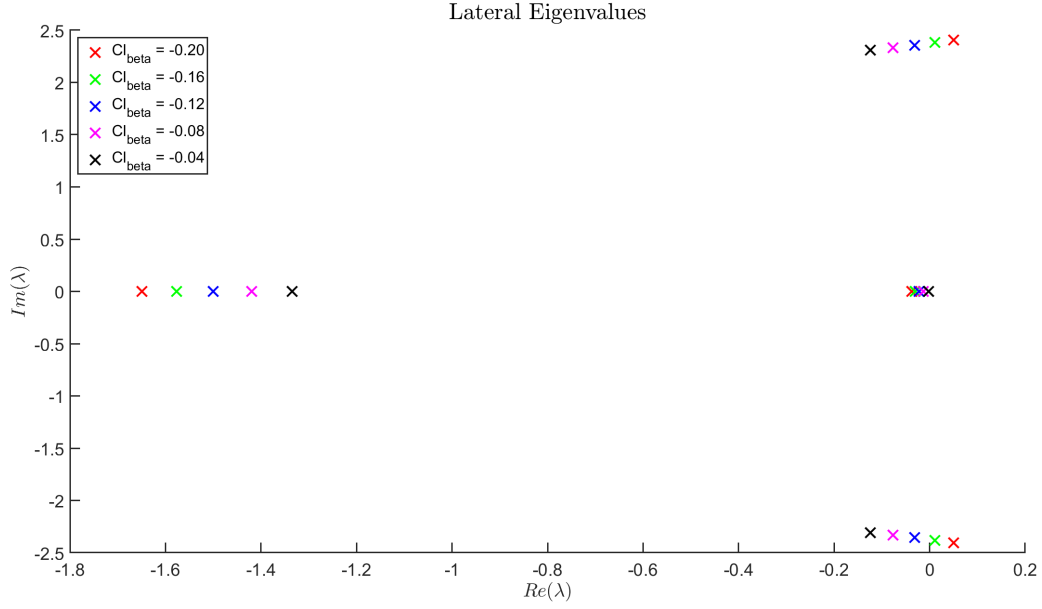


Figure 22: Effect of $C_{l_{\beta}}$ on lateral-directional dynamics

Figures 22 and 23 show the lateral-directional eigenvalues plotted for different values of $C_{l_{\beta}}$ and C_{n_r} respectively. It can be observed that an increase in the magnitude of $C_{l_{\beta}}$ stabilizes the roll and spiral modes, but the dutch-roll mode becomes unstable. This is an effect of the roll stability significantly outweighing the yaw stability. On the other hand, increasing the magnitude of C_{n_r} the dutch-roll and spiral modes while having insignificant effect on the roll dynamics.

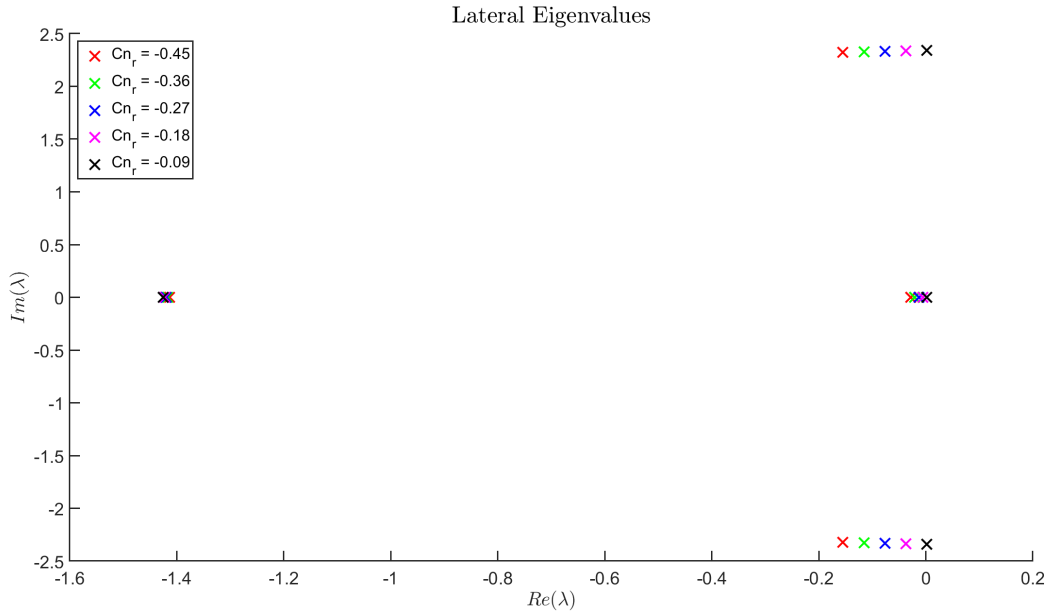


Figure 23: Effect of C_{n_r} on lateral-directional dynamics

12 Transfer Functions

Note that the control inputs here are perturbations on the trim control inputs and the responses are also perturbations on the trim states.

12.0.1 Elevator Deflection Input

$$\text{Ge2u} = \frac{4.19s^3 + 129.1s^2 + 142.8s + 51.02}{s^4 + 1.001s^3 + 7.629s^2 + 0.0689s + 0.02124}$$

$$\text{Ge2w} = \frac{-14.02s^3 - 2765s^2 - 18.73s - 5.641}{s^4 + 1.001s^3 + 7.629s^2 + 0.0689s + 0.02124}$$

$$\text{Ge2q} = \frac{-10.72s^3 - 5.266s^2 - 0.03633s - 3.468 \times 10^{-18}}{s^4 + 1.001s^3 + 7.629s^2 + 0.0689s + 0.02124}$$

$$\text{Ge2}\theta = \frac{-10.72s^2 - 5.266s - 0.03633}{s^4 + 1.001s^3 + 7.629s^2 + 0.0689s + 0.02124}$$

12.0.2 Throttle setting input

$$\text{Gt2u} = \frac{5.653 \times 10^{-5}s^3 + 5.619 \times 10^{-5}s^2 + 0.00043s - 7.197 \times 10^{-7}}{s^4 + 1.001s^3 + 7.629s^2 + 0.0689s + 0.02124}$$

$$\text{Gt2w} = \frac{-2.955 \times 10^{-6}s^2 + 1.75 \times 10^{-5}s - 3.268 \times 10^{-8}}{s^4 + 1.001s^3 + 7.629s^2 + 0.0689s + 0.02124}$$

$$\text{Gt2q} = \frac{7.344 \times 10^{-8}s^2 + 1.229 \times 10^{-7}s + 5.544 \times 10^{-27}}{s^4 + 1.001s^3 + 7.629s^2 + 0.0689s + 0.02124}$$

$$\text{Gt2}\theta = \frac{7.344 \times 10^{-8}s + 1.229 \times 10^{-7}}{s^4 + 1.001s^3 + 7.629s^2 + 0.0689s + 0.02124}$$

12.0.3 Aileron Deflection Input

$$\text{Ga2v} = \frac{0.5679s^3 - 134s^2 - 180s - 21.73}{s^4 + 1.542s^3 + 6.417s^2 + 7.232s + 0.08423}$$

$$\text{Ga2p} = \frac{-9.187s^3 - 3.169s^2 - 45.75s + 0.07856}{s^4 + 1.542s^3 + 6.417s^2 + 7.232s + 0.08423}$$

$$\text{Ga2r} = \frac{0.1055s^3 + 0.2702s^2 - 2.029s - 1.73}{s^4 + 1.542s^3 + 6.417s^2 + 7.232s + 0.08423}$$

$$\text{Ga2phi} = \frac{-9.182s^2 - 3.157s - 45.84}{s^4 + 1.542s^3 + 6.417s^2 + 7.232s + 0.08423}$$

12.0.4 Rudder Deflection Input

$$\text{Gr2v} = \frac{3.372s^3 + 694.2s^2 + 816.9s - 7.139}{s^4 + 1.542s^3 + 6.417s^2 + 7.232s + 0.08423}$$

$$\text{Gr2p} = \frac{1.54s^3 - 0.6694s^2 - 38.78s + 0.06677}{s^4 + 1.542s^3 + 6.417s^2 + 7.232s + 0.08423}$$

$$\text{Gr2r} = \frac{-2.603s^3 - 3.324s^2 - 1.981s - 1.47}{s^4 + 1.542s^3 + 6.417s^2 + 7.232s + 0.08423}$$

$$\text{Gr2phi} = \frac{1.422s^2 - 0.8203s - 38.87}{s^4 + 1.542s^3 + 6.417s^2 + 7.232s + 0.08423}$$

13 Response to Elevator Deflection

The following plots show response of aircraft Simulink model to 1 deg step deflection in elevator from the trim position. The step deflection takes place at 10s and the simulation is run for 265.4s

13.1 Δu Response

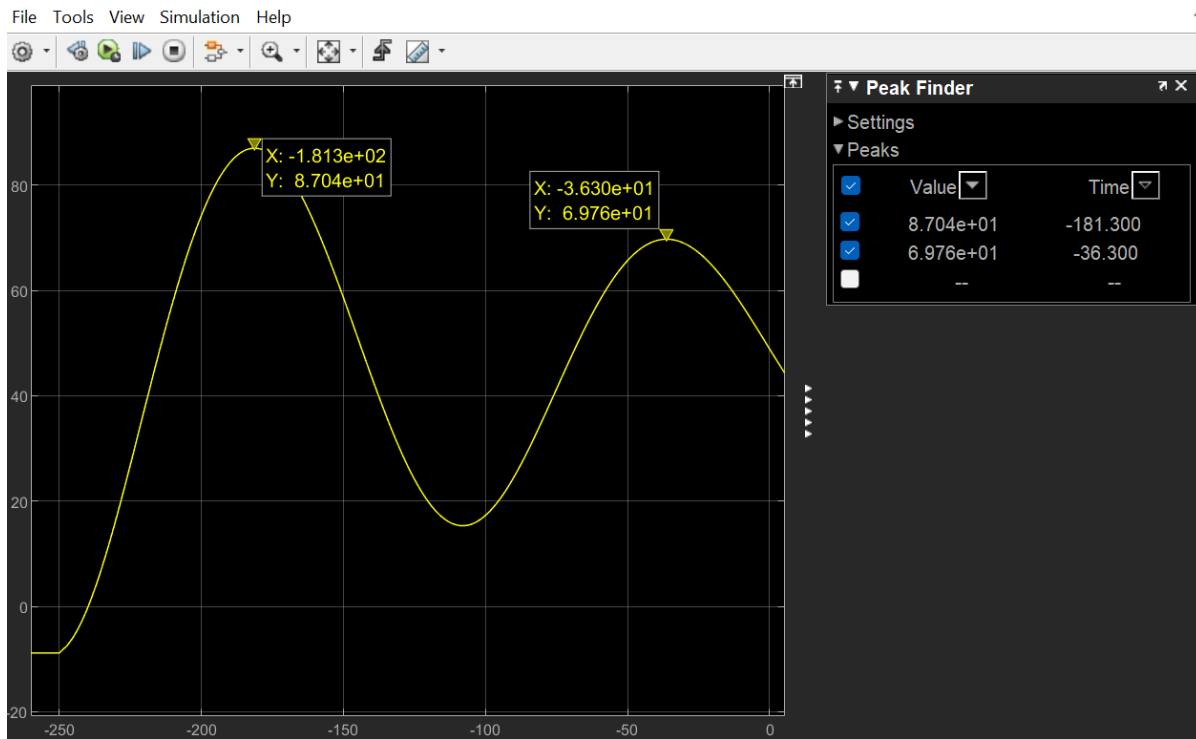


Figure 24: $\Delta u(t)$

13.2 $\Delta\gamma$ Response

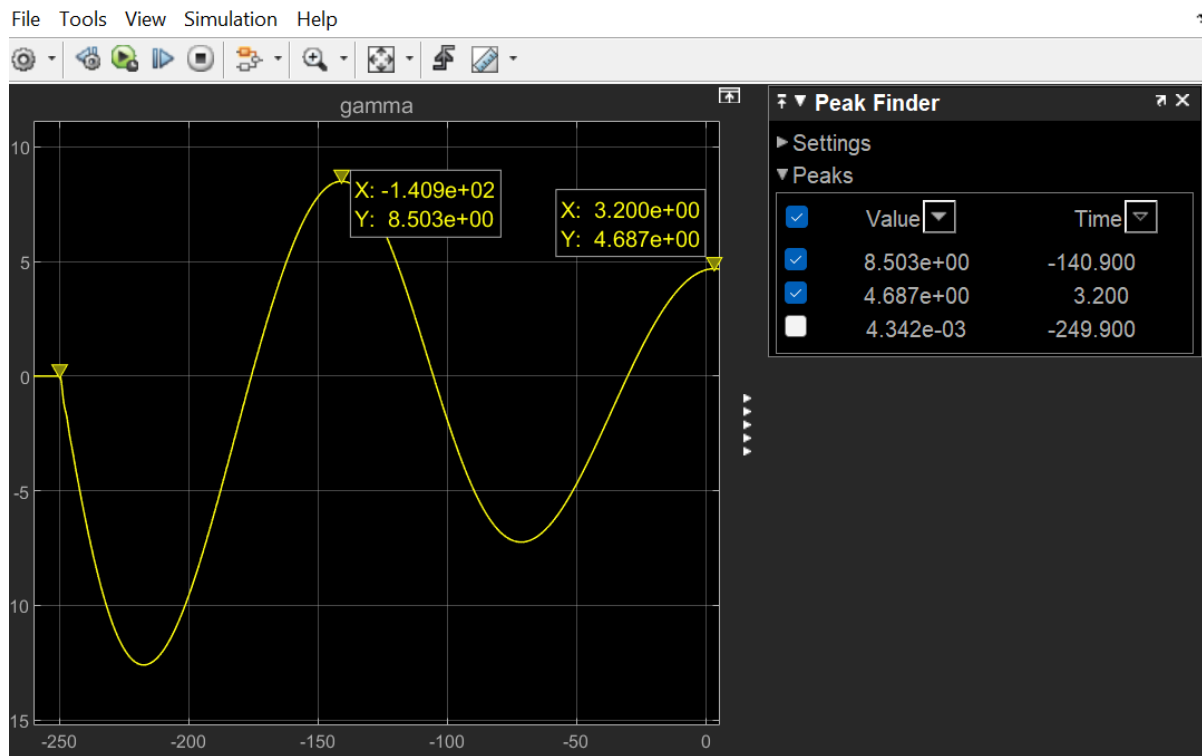


Figure 25: $\Delta\gamma(t)$

Note there is no significant short term response. Phugoid mode is dominant in delta u and delta gamma response.

13.3 α Response

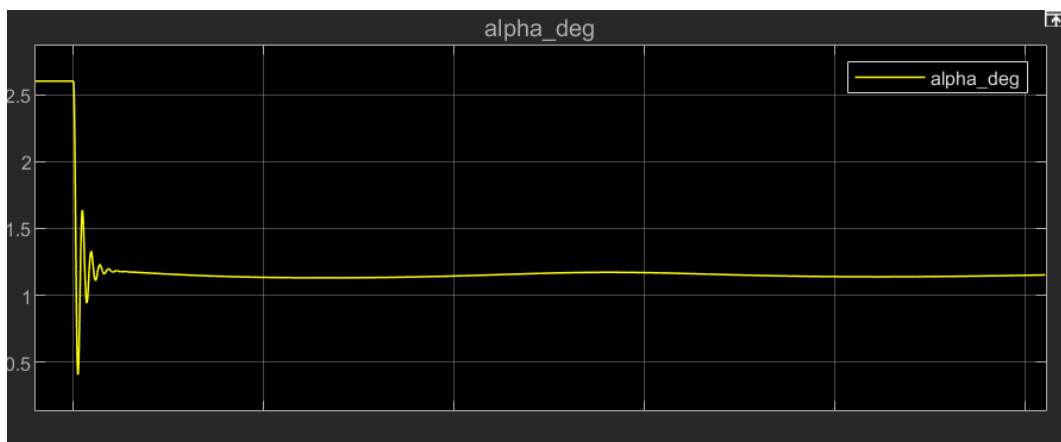


Figure 26: $\alpha(t)$ Long Term

13.4 $\Delta\theta$ Response

13.4.1 Long Term Response

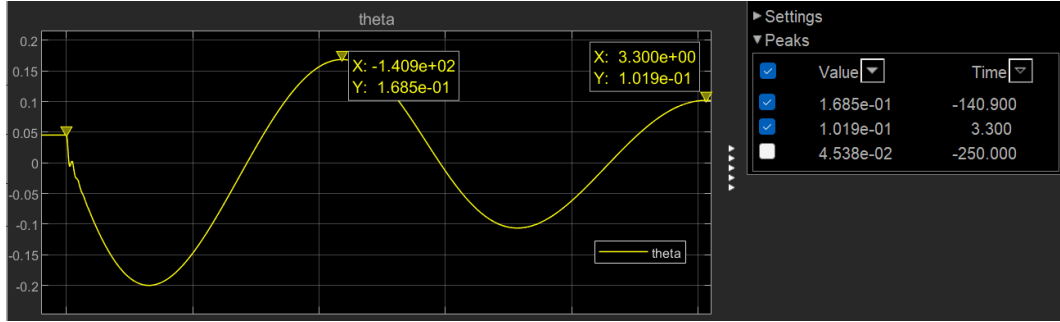


Figure 27: $\Delta\theta(t)$ Long Term

13.4.2 Short Term Response

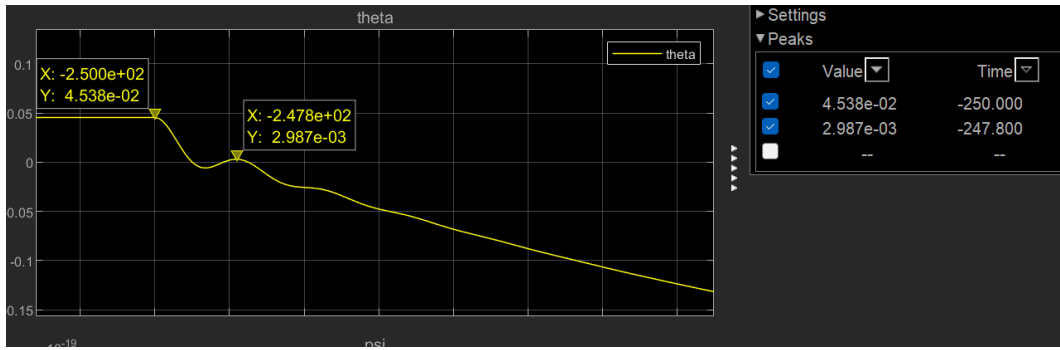


Figure 28: $\Delta\theta(t)$ Short Term

Note that long term response shows effect of phugoid while the short term response shows that there is fast decaying oscillations which corresponds to the short period mode. Similar response can be seen in the delta q response

13.5 Δq Response

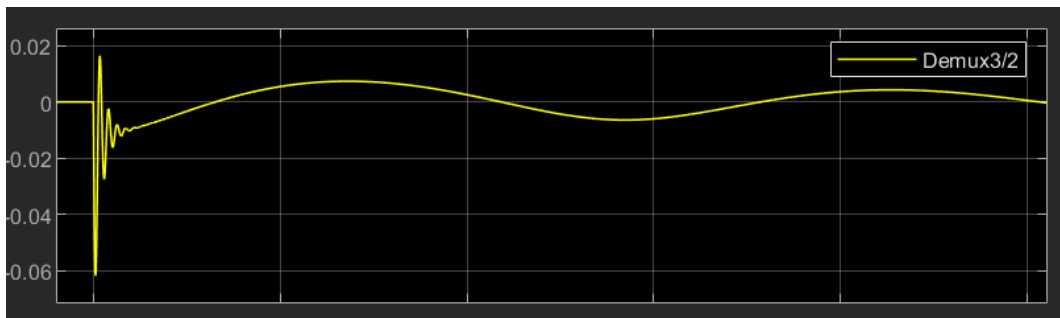


Figure 29: $\Delta q(t)$

13.6 MATLAB Transfer Function Responses

Plotting responses based on the transfer functions we have derived for the linearised model at the trim operating condition.

Here the deflection starts at 100s and the simulation stop time is 1000s

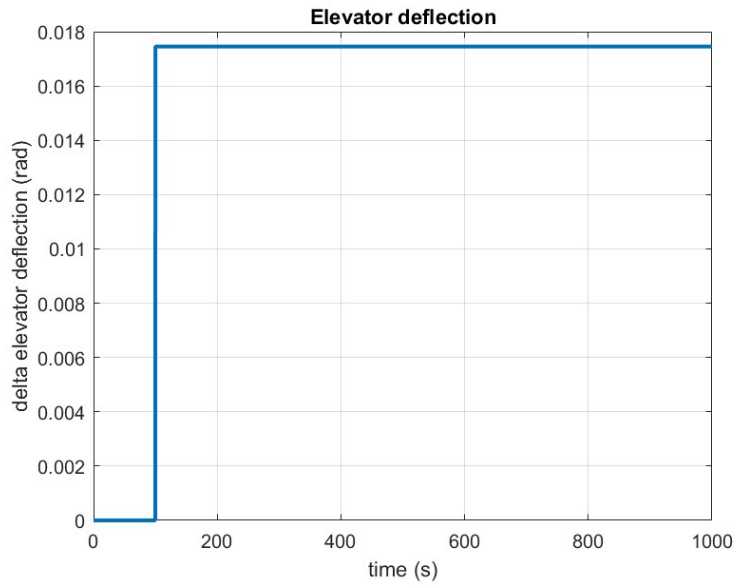
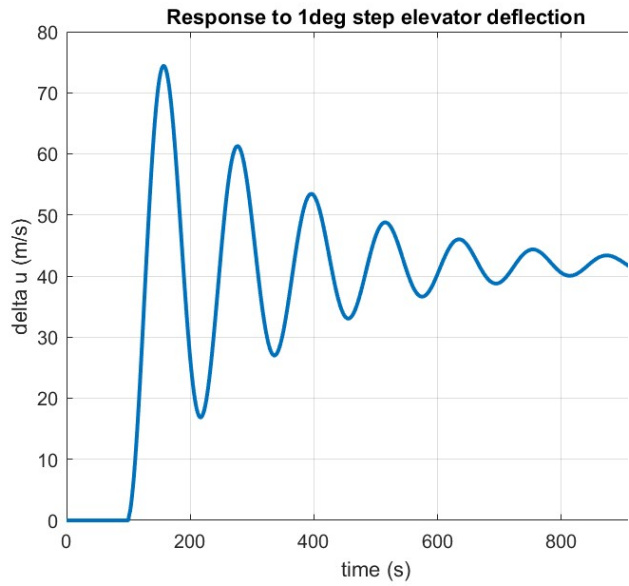
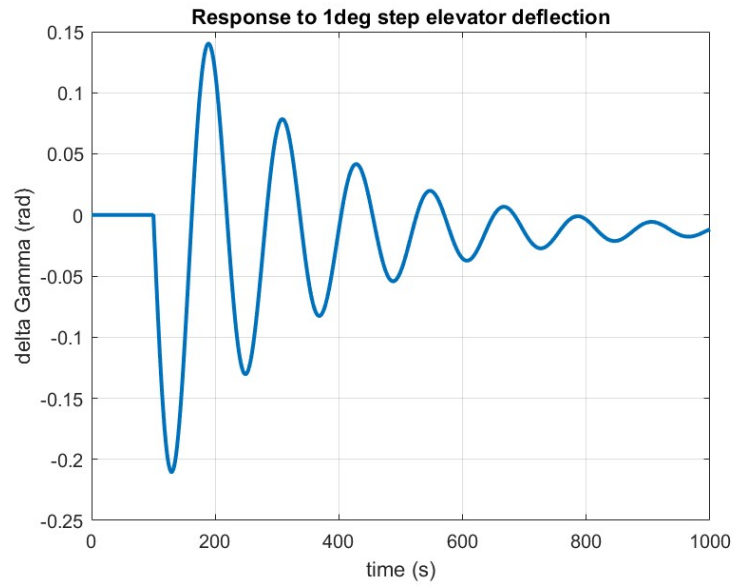


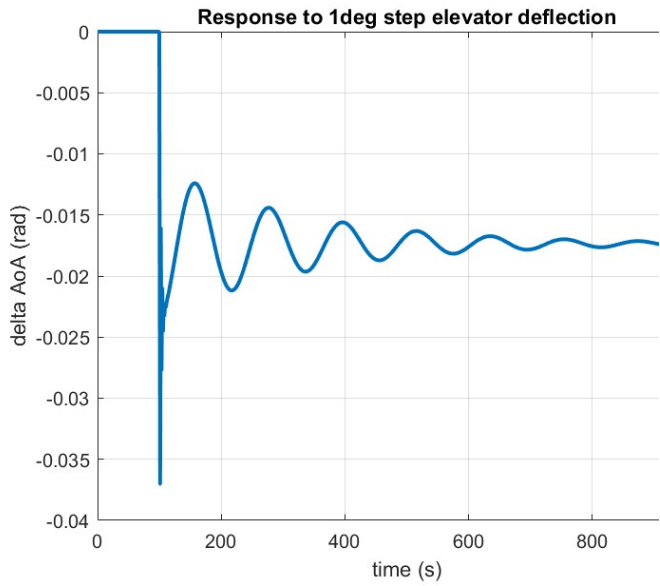
Figure 30: $\Delta\delta_e(t)$



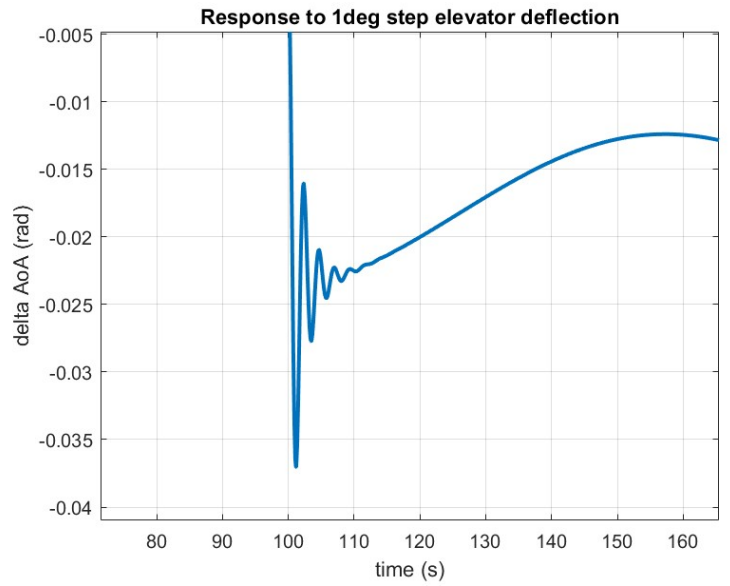
(a) $\Delta u(t)$



(b) $\Delta\gamma(t)$



(a) $\Delta\alpha(t)$ Long term



(b) $\Delta\alpha(t)$ Short term

We can observe that there are two different transients one is a large amplitude slow oscillation which corresponds to the phugoid mode and then there is a faster much smaller transient due to the Short Period mode seen in delta alpha.

These plots were obtained using the `lsim` function of MATLAB with transfer functions obtained earlier and a custom mad step input. This shows the expected open loop response of plant when we design our Autopilot based on the control model.

14 Response to Aileron Deflection

a -15° step response was subjected to the plant and the response of (u,v,w) velocity in body frame, (p,q,r) body angular rates and (ϕ, θ, ψ) were plotted.

In the Simulink model I added a step response of -15° in aileron deflection. The aircraft crashes into the ground at 58.156s.

14.1 Velocity Response

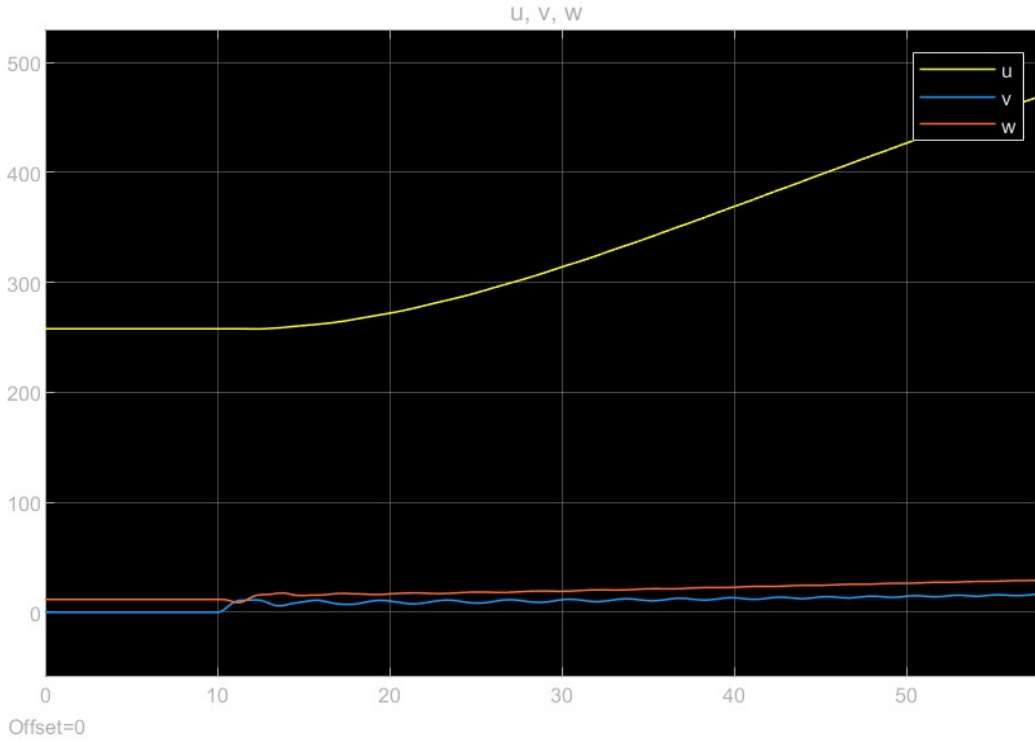
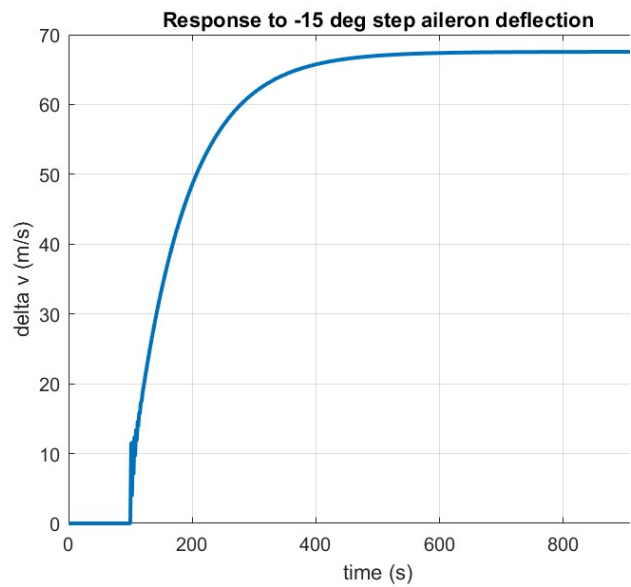


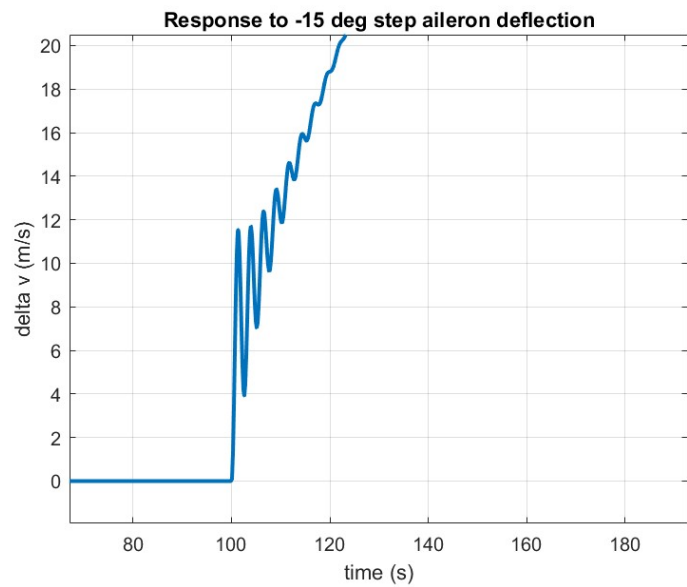
Figure 33: Velocity components in body frame

$\delta v(t)$ expected from transfer function relating aileron deflection to δv looks like a first order response so we believe that it is being dominated by a slow first order system which is the Spiral Mode

The δv response shows comparatively faster transient oscillations at start which corresponds to Dutch Roll mode. Note that an aileron deflection will excite all the lateral longitudinal modes, there will not be any pure modal response.



(a) $\Delta v(t)$



(b) $\Delta v(t)$ Short Term

14.2 Body Angular Rates Response

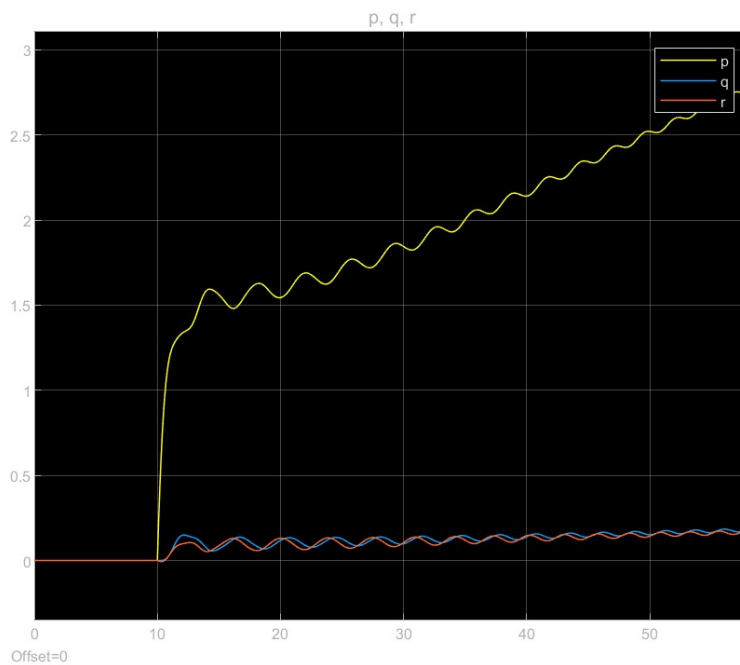
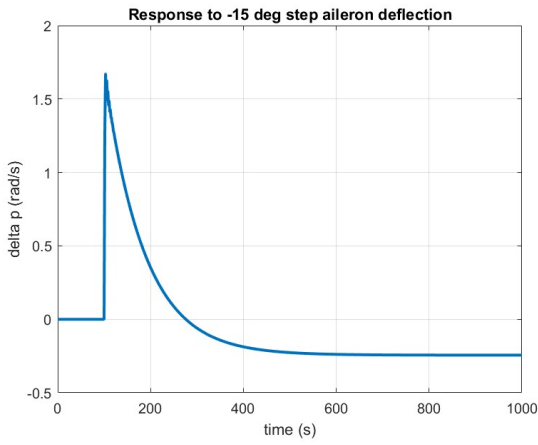
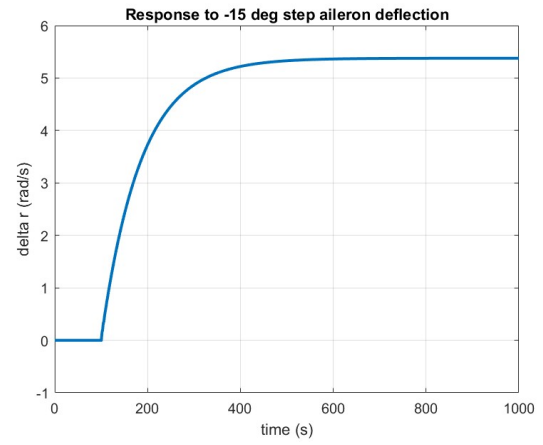


Figure 35: Body angular rate components in body frame



(a) $\Delta p(t)$



(b) $\Delta r(t)$

14.3 Attitude angles Response

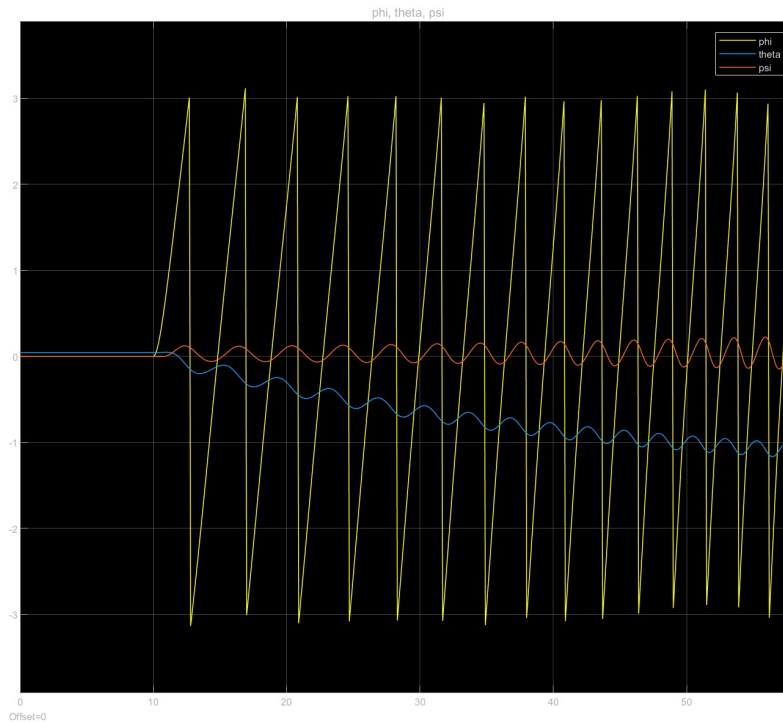


Figure 37: attitude angles

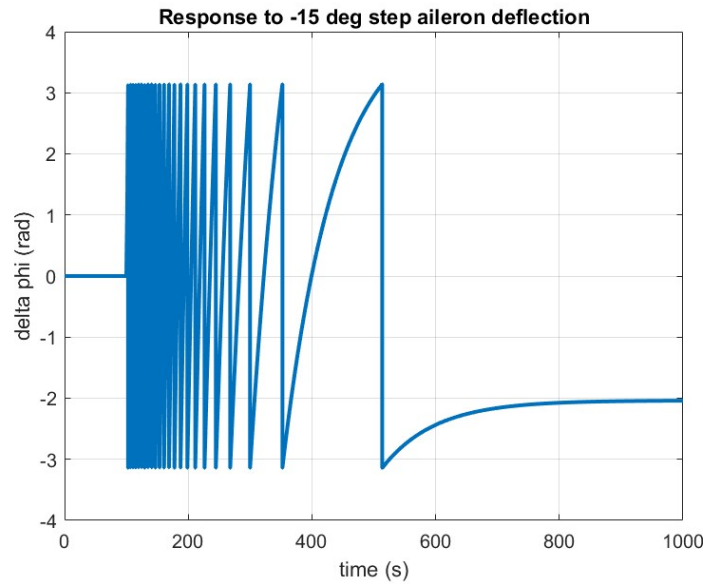


Figure 38: $\Delta\phi(t)$

This seems to have oscillations because phi is wrapped between 0 to pi

15 Conclusion

The full 12 state linearised state space representation was decoupled into longitudinal and lateral-directional dynamics. The eigen values of the system A matrix gave us the poles of the system which corresponds to the dynamic modes of the aircraft. Longitudinal system contained a set of 2 oscillatory poles for Phugoid and Short-Period Mode and the Lateral-Directional Dynamics had 2 real poles corresponding to roll subsidence and spiral mode and an oscillatory pole representing Dutch Roll mode.

From the eigen values we were able to observe that the aircraft without an autopilot is stable for small perturbations about the trimmed condition. but the poles for phugoid and spiral are indeed very close to the origin. Varying the stability derivatives we could see the shift in poles and relate it back to theoretical understanding of which stability derivative affects which mode. Step deflections to elevator and ailerons was given in the model and we observed the effect it has on the flight.

An actuator block was implemented and using Simulink's Joystick input block we could actually pilot the aircraft in the simulation model. The future plan is to use the reduced order control model to design autopilot loops and then implement controllers with the same gain in the simulation model and observe the effects and handling quality while flying.

References

- [1] Airplane Flight Dynamics and Automatic Flight Controls, Jan Roskam
- [2] Small Unmanned Aircraft, Randall Tim
https://github.com/randybeard/mavsim_public
- [3] Aircraft Flight Mechanics Notes, Harry Smith
<https://www.aircraftflightmechanics.com/NotesIntroduction.html>
- [4] Coupling Dynamics in Aircraft: A Historical Perspective, Richard E. Day
<https://ntrs.nasa.gov/api/citations/19970019603/downloads/19970019603.pdf>